

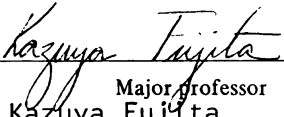
This is to certify that the
thesis entitled

INTRAPLATE SEISMICITY IN
CENTRAL ALASKA AND CHUKOTKA

presented by
Michael J. Coley

has been accepted towards fulfillment
of the requirements for

M.S. degree in Geological Sciences


Major Professor
Kazuya Fujita

Date 8 August, 1983



RETURNING MATERIALS:
Place in book drop to
remove this checkout from
your record. FINES will
be charged if book is
returned after the date
stamped below.

~~APR 05 1990~~
M019480
9-82

~~ROOM USE ONLY~~

~~ROOM USE ONLY~~

INTRAPLATE SEISMICITY IN
CENTRAL ALASKA AND CHUKOTKA

by

Michael J. Coley

A THESIS

Submitted to

Michigan State University

in partial fulfillment of the requirements

for the degree of

MASTER OF SCIENCE

Department of Geological Sciences

1983

154-0713

ABSTRACT

INTRAPLATE SEISMICITY IN
CENTRAL ALASKA AND CHUKOTKA

BY

MICHAEL J. COLEY

Central Alaska and Chukotka (northeasternmost Siberia) exhibit high levels of seismicity. The area is relatively far from present day plate boundaries and lacks an easily identifiable source for the earthquakes. A study of the areas largest magnitude events was undertaken to define a regional model which would explain the anomalous seismic activity. Focal mechanisms were constrained for twelve earthquakes and an additional four mechanisms were obtained from previously published data. Normal and strike-slip faulting mechanisms were found to be more predominant in western Alaska and the Bering Sea while reverse and strike-slip mechanisms were prevalent in central Alaska. This suggests that the stress regime changes from primarily extensional in the Bering Sea to compressional in central Alaska. In addition, the majority of the earthquakes occurred on pre-existing faults.

ACKNOWLEDGEMENTS

I must thank my wife for the vast amount of moral support and understanding she freely gave. She forgave me for the many times when I was not there and for my all too common bad moods and anxiety attacks during the few times we were together. She also put many hours into the preparation of this thesis. If Terri was the moral support than Kaz handled the technical end of things. I can remember about six months of late nights and early mornings he spent helping me with the never ending computer problems, program bugs, technical questions, etc... which constantly plagued me. His comments on the thesis were concise and to the point. I know that his thoroughness took him many extra hours and saved me valuable time. I must also thank Martha for her corrections on my marginal spelling and English. A pair of people who also bear mention are my parents who put up with me during some difficult years in high school. Their faith and financial support saw me through times when a degree seemed unobtainable. Four others who bear mentioning are Newberry, Dave L., Dave P. and Bruce for the many hours of discussion and friendship. It made the hard times more easy to bear. Lastly, I must thank Michigan State University and the Department of Geological Sciences for the use of their equipment and financial assistance. This research was supported in part by NSF grant EAR-8025267.

TABLE OF CONTENTS

Introduction.....	1
Methodology.....	6
First motion plots.....	6
Rayleigh wave radiation patterns.....	7
Fault plane determination.....	10
Geology.....	14
Seward Peninsula.....	14
Western Brooks Range.....	17
Yukon-Koyukuk Province.....	17
Ruby Geanticline.....	18
Central Alaska.....	18
Chukotka.....	19
Southern Hope Basin.....	19
Seismicity.....	20
Seward Peninsula.....	20
Yukon-Koyukuk Province.....	21
Western Brooks Range.....	25
Central Alaska.....	25
Chukotka and Southern Hope Basin.....	26
Areas of No Seismicity.....	26
Focal Mechanisms.....	29
Rampart Series (Event 1).....	29

TABLE OF CONTENTS
(continued)

Chukotka Earthquake (Event 6).....	45
Seward Peninsula (Event 7).....	51
Event 8.....	55
Events 9 and 10.....	57
Events 11 and 12.....	61
Huslia Series (Events 13 and 14) and Event 15.....	64
Caro (Event 16).....	74
Discussion.....	80
Conclusions.....	92
Bibliography.....	93

LIST OF FIGURES

1. Teleseismic earthquake epicenters in the study area.....	2
2. Theoretical Love and Rayleigh wave radiation patterns.....	11
3. Index map of the study area.....	16
4A. Seismicity of Western Alaska: Epicentral locations.....	23
4B. Seismicity of Western Alaska: Relation of earthquakes to structural features.....	24
5. Chukotka epicenters.....	27
6. First motion data of event 1.....	31
7. Rayleigh wave radiation pattern of event 1.....	33
8. Gedney (1970) data for event 1.....	34
9. Aftershock relocation for event 1.....	35
10. Final mechanism for event 1.....	37
11. First motion data of event 2.....	38
12. First motion data of event 3.....	39
13. First motion data of event 4.....	41
14. First motion data of event 5.....	42
15. Structural features near the Rampart series.....	44
16. Model of Weaver and Hill (1978/79).....	46
17. Rayleigh wave radiation pattern of event 6 before station deletion.....	47
18. Rayleigh wave radiation pattern of event 6 after station deletion.....	48
19. First motion data for event 6.....	50
20. First motion data for event 7.....	52

LIST OF FIGURES (continued)

21.	Rayleigh wave radiation pattern of event 7 before station deletion.....	53
22.	Rayleigh wave radiation pattern of event 7 after station deletion.....	54
23.	Final mechanism for event 7.....	56
24A.	Focal mechanism solution for event 8: after Sykes and Sbar (1974).....	58
24B.	after Liu and Kanamori (1980).....	58
25.	First motion data of event 9.....	59
26.	Aftershock relocation of event 9.....	60
27.	First motion data of event 10.....	62
28.	Composite first motion data of events 11.....	63
29.	First motion data of event 12.....	65
30.	First motion data of event 14 from the ISS.....	66
31.	First motion data of event 13 from the ISS.....	67
32.	Proposed mechanisms for event 13.....	70
33.	First motion and S-wave polarization angle data of event 13.....	71
34.	First motion data of event 15.....	73
35.	Rayleigh wave radiation pattern for event 16.....	75
36.	First motion data of event 16.....	76
37.	Seismic record at station "COL" for event 16.....	78
38.	Focal mechanism distribution.....	81
39.	Maximum horizontal compression (MHC) from Nakamura and Uyeda (1980).....	86
40.	MHC orientations from focal mechanisms.....	89

LIST OF TABLES

List of Events.....	4-5
List of Focal Mechanisms.....	82-83

INTRODUCTION

In general, plate tectonic theory states that earthquakes occur as a result of interactions between rigid pieces of the lithosphere as they collide, pull apart, and slide past each other. This explains the high level of seismic activity which is observed along the boundaries of the plates. However, there are many areas far removed from plate boundaries which also exhibit high levels of seismicity; for example, eastern and central North America (Zoback and Zoback, 1980), the central Indian Ocean (Stein and Okal, 1978), Australia, and Africa (Sykes, 1978). These seismically active intraplate regions are not explained by general plate tectonic theory. An increasing amount of research has been directed toward such areas (Sykes and Sbar, 1974; Richardson et al., 1976; Wang et al., 1979; Liu and Kanamori, 1980). Such studies have helped to define the intraplate stress regime, zones of weakness within the plates, and present day tectonic activity.

Central Alaska and Chukotka (northeast corner of Siberia) is another intraplate area which exhibits anomalous high levels of seismic activity. A map of epicentral locations is shown in Figure 1. Data for this were obtained from the International Seismological Center (ISC) Bulletin (1964-1981), the International Seismological Summary (ISS) from 1904 to 1963, Seismic Zoning of the USSR (Goryachev et al., 1968), Novii Katalog Sil'nikh Zemletryasenii. na Territorii SSSR (Kondorskaya and Shebalin, 1977) and the National Oceanic and Atmospheric Administration (NOAA)

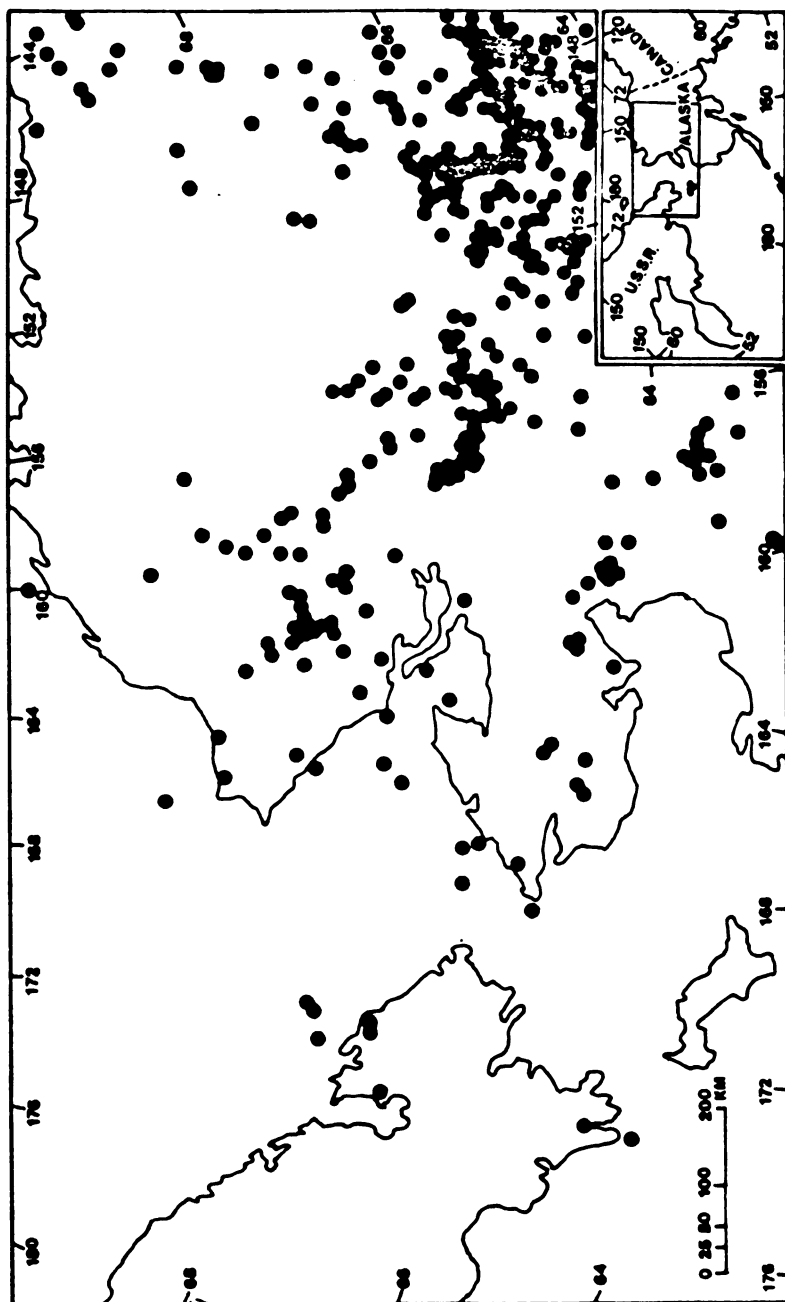


FIGURE 1
TELESEISMIC EARTHQUAKE EPICENTERS IN THE STUDY AREA

United States Earthquake publication (1928-1963). The area has long been recognized as a zone of intraplate seismicity. However, most authors have either studied the effects of individual events (Bramhall, 1938; St. Amand, 1948; Davis, 1960) or have focused on the southern portion of Alaska (Gedney and Berg, 1969a,b; Gedney, 1970; VanWormer et al., 1974; Bhattacharya and Biswas, 1979).

The purpose of this research was to determine the cause of the intraplate earthquakes in central Alaska and Chukotka. Focal mechanisms were constrained for twelve of the area's largest magnitude events. An additional four mechanisms were obtained from previously published data. A list of the earthquakes used is shown in Table 1. Each event was studied individually to determine whether it occurred on existing faults or structural features. A regional study of all events was done in order to explain the areal distribution of the observed focal mechanisms. The findings of this research support the studies of Nakamura et al. (1977, 1980) that compressional stresses are dominant in central and southern Alaska, while primarily tensional stresses exist in western Alaska and the Bering Sea.



TABLE 1

LIST OF EVENTS

Event Number	Date & Time		Epicenter		Magnitude (M_b) unless noted	Number of Stations Reporting	References
	(Yr-Mn-Da)	Hr.Mn.Sec)	LAT(N)	LONG(W)			
1	68-10-29	22.16.16	65.46	150.07	6.0	312	Gedney, 1970
2	68-11-03	07.37.39	65.74	149.86	4.4	51	
3*	73-05-07	17.39.46	65.04	150.00	3.4(M_L)	16	Bhattacharya and Biswas, 1979
4	61-01-30	12.12.36	65.2	150.2	5.5	82	
5*	67-06-21	18.04.50	64.8	147.4	5.4	211	Gedney, 1970
6	71-10-05	01.40.41	67.38	172.57	5.2	133	
7	64-12-13	00.33.27	64.88	165.57	5.3	131	
8*	65-04-16	23.22.18	64.69	160.23	5.8	191	Sykes and Sbar, 1974, Liu and Kanamori, 1980
9	81-07-12	01.27.56	67.71	161.20	5.2	161	
10	66-08-26	10.19.32	66.71	162.7	5.0	82	
11	52-11-21	17.26.50	66.2	167.1	N.A.	33	
	52-12-28	04.55.12	65.9	167.00	N.A.	99	
	60-07-16	21.19.39	65.9	167.00	N.A.	70	
	60-07-16	22.02.54	65.74	166.95	N.A.	55	
12	64-06-11	03.11.58	65.35	168.3	5.0	61	

TABLE 1
(continued)

Event Number	Date & Time (Yr-Mn-Da Hr.Mn.Sec)	Epicerter LAT(N) LONG(W)	Magnitude (Mb) unless noted	Number of Stations Reporting	References
13*	58-04-07 15.30.40	66.03 156.59	7.3	350	Schaffner, 1961 Balakina, 1962 Ritsema, 1962 Stevens, 1964
14	58-04-13 09.07.24	66.00 156.00	6.5	171	
15	58-05-10 22.54.39	65.23 152.1	6.3	163	
16	66-12-20 00.26.28	66.82 148.1	4.8	69	
	66-12-20 00.57.53	66.79 148.4	4.9	82	

* - focal mechanism is not constrained within this study

N.A. - magnitude data for these events are not available

METHODOLOGY

This research is based upon the focal mechanisms of 16 earthquakes which occurred in central Alaska and the southern Chukchi Sea (Table 1). Of the 16 mechanisms used, 12 were constrained within this study. These 12 events were chosen from the ISC Bulletin and the ISS on the basis of magnitude. Larger magnitude events create larger amplitude seismic waves, thus they are recorded by more seismic observatories and are more easily studied. Focal mechanisms were constrained using first motion data and Rayleigh wave amplitude vs. azimuth plots. Once a mechanism was constrained, the fault plane was determined if possible by geological criteria and, for those events exhibiting foreshock and/or aftershock sequences, alignment of earthquake epicenters.

First Motion Plots

The polarity of the first motions were plotted for all of the events included in this study. Often, the first motion plots constrained the nodal planes well enough to give a good focal mechanism. The plotting method used in this research is described by Herrmann (1975) and is outlined below.

The short and long period vertical component seismograms were studied to obtain the "first motion", whether it is up (compressional) or down (dilatational), of the P-wave. This data set was supplemented with first motions reported in the ISS for earthquakes occurring between 1933

and 1964 and from the ISC Bulletin for events occurring since 1964. The P-wave takeoff angle at the hypocenter, which is a function of focal depth and epicentral distance, is obtained from Pho and Behe (1972). The first motion polarity is then plotted on an equal-area stereonet as a function of station azimuth, marked on the perimeter of the stereonet, and takeoff angle, which is measured as degrees from the downward vertical. The first motions will ideally divide the focal sphere (an imaginary sphere surrounding the earthquake hypocenter) into four quadrants. The quadrants are separated by two mutually perpendicular nodal planes. These are planes along which no P-wave energy is radiated.

In practice, the nodal planes will not divide the focal sphere into quadrants which contain only compressions or dilations. There are almost always a few compressions in with the dilations and vice-a-versa due to noise and operator error. However, in many cases (particularly for strike-slip mechanisms), the nodal planes can be constrained well enough to enable a good focal mechanism determination.

Rayleigh Wave Radiation Patterns

Further constraints were made on the focal mechanisms of four of the events by calculating their Rayleigh wave radiation patterns. Records from the World Wide Standardized Seismograph Network (WWSSN) are used in the computations. The WWSSN is a network of seismic observatories which use a standardized system of recording instruments and has been in operation since 1964. This enables a standardized set of earthquake recordings for events occurring since 1964 to be easily obtained. Records from earthquakes which occurred prior to 1964 are difficult to find and were recorded by instruments set to variable specifications. Thus,

Rayleigh wave radiation patterns were not attempted on any pre-1964 earthquakes. In addition, only larger magnitude events ($M_b 5.0$) can be used, as smaller magnitude earthquakes do not release enough energy to enable propagation of surface waves over large distances. Thus, a sufficient number of earthquake recordings are not available to calculate a reliable radiation pattern. This method is also applicable to Love wave data. However, recordings of Rayleigh waves are usually better than those for Love waves and should give more accurate results. In addition, Rayleigh waves do not have to be corrected for polarization angle as do Love waves.

The Frequency spectrum, (ω) for a seismogram, where ω is frequency, is given by Kanamori and Stewart (1976) as:

$$X(\omega) = \frac{1}{\sqrt{\sin\theta}} e^{-\frac{i\pi}{4}} e^{-\frac{i\omega a\theta}{C}} \{P_L P_L^{(1)} + q_L Q_L^{(1)}\} e^{-\frac{\omega\theta a}{2QU}}$$

where θ = angular distance from the earthquake
 a = earth's radius
 C = phase velocity (km/sec)
 U = group velocity (km/sec)
 Q = quality factor (attenuation)

The decaying exponential term,

$$e^{-\frac{\omega\theta a}{2QU}}$$

shows that the signal is attenuated. The complex exponential,

$$e^{-i\omega a\theta/C}$$

gives the phase as a function of position. The square root term,

$$1/\sqrt{\sin\theta}$$

takes account for geometrical spreading. The term in brackets contains the azimuthal variation due to the radiation pattern and the amplitude. The terms are as follows:

$$P_L = \cos\delta \sin\lambda \sin\delta \sin 2(\phi_f - \phi) + \cos\lambda \sin\delta \cos(\phi_f - \phi)$$

$$Q_L = \cos\lambda \cos\delta \sin(\phi_f - \phi) + \sin\lambda \cos 2\delta \cos(\phi_f - \phi)$$

The $P_L^{(1)}$ and $Q_L^{(1)}$ terms account for the frequency and the elastic constants. The last four terms are radiation terms and allow the computation of the amplitude radiation pattern at a given frequency (Kanamori and Stewart, 1976) by use of the equation:

$$A(\phi) = \sqrt{(P_L P_L^{(1)})^2 + (Q_L Q_L^{(1)})^2}$$

The pattern will depend upon the fault geometry: strike θ_f , dip δ , and slip λ .

An equalization term is used in the calculation to account for the difference in source-station distances (Kanamori, 1970) and is:

$$X(\theta_o, \omega) = \sqrt{\frac{\sin\theta}{\sin\theta_o}} X(\theta, \omega) e^{i\left\{\frac{\omega a(\theta - \theta_o)}{C} - \frac{\pi}{2}M\right\}} e^{\frac{\omega a(\theta - \theta_o)}{2QU}}$$

The M term accounts for higher order surface wave trains. These computations were performed using a program written by Seth Stein of Northwestern University.

Rayleigh waves from WWSSN station recordings were digitized. These data were converted to the frequency domain using Fourier transforms. The average spectral amplitude can then be calculated over a specific frequency range. This study uses frequency values from .033 Hz (30 sec. period) to .0143 Hz (70 sec. period). The spectral amplitudes for each station's recordings are corrected to a common station magnification (1500) and distance from the source (90 degrees). The final output is a plot for each station's wave amplitude vs. the station azimuth from the earthquake epicenter for a specific frequency band. The theoretical

radiation pattern depends on the fault geometry; that is, the fault strike, dip, and slip angle. Ideal radiation patterns, assuming the earthquake energy is propagated uniformly in all directions, are shown in Figure 2 for four different fault geometries. In practice, the observed pattern is more jagged. This is due primarily to irregularities in the earth's crustal structure. The actual fault parameters are constrained by allowing the program to calculate a theoretical pattern for a given set of fault parameters; theoretical and observed patterns are then superimposed. The correct parameters are those of the theoretical pattern which most closely agree with the observed pattern.

The program also calculates a record's amplitude spectrum which can be used as a quality check on recordings from individual stations. Since WWSSN instruments have peak periods of 20 seconds, many records which show numerous spurious amplitude peaks are questionable.

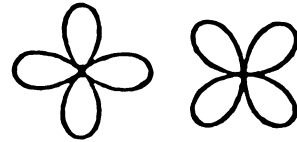
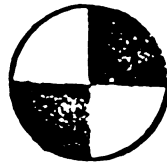
Fault Plane Determination

Once a focal mechanism is constrained for a given earthquake, it must be determined which of the nodal planes is the fault plane. This will be the one on which movement has occurred. If the earthquake occurs as either a single event or as an earthquake pair, the fault plane is most easily obtained by a study of the nearby geology and structure. If fault trends or the structural grain near an earthquake epicenter parallel one of the nodal planes, then that plane is chosen to be the fault plane.

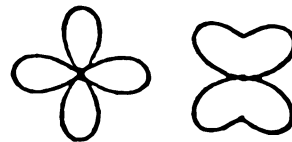
However, two of the earthquakes studied were large magnitude events which were either preceded and/or followed by many smaller magnitude events (see Table 2). These series of smaller magnitude earthquakes are referred to as foreshock or aftershock sequences. If the epicenters

SURFACE WAVE RADIATION PATTERN

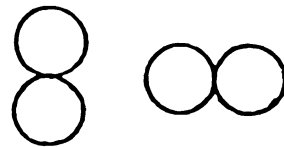
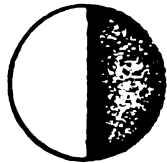
VERTICAL
STRIKE SLIP



45°
STRIKE SLIP



VERTICAL
DIP SLIP



45°
DIP SLIP



LOVE RAYLEIGH

FIGURE 2

THEORETICAL LOVE AND RAYLEIGH WAVE RADIATION PATTERNS

of a foreshock and/or aftershock series tend to align in a well defined trend, and if the trend parallels one of the nodal planes, then that plane is the likely fault plane. It is possible to use epicentral locations published in the ISC Bulletin for the determination of such a trend. The problem lies in the ISC's epicentral location method. The method uses reported arrival times to determine earthquake hypocentral locations. It also assumes a spherically symmetric earth model in its location program which does not take into account lateral crustal and mantle inhomogeneities. The inhomogeneous nature of the earth will cause the actual travel time for a ray traveling between a specific source-receiver pair to be different than the ideal travel time of a ray in the symmetrical earth model for the same source-receiver pair. The difference between the actual and ideal travel time is called the residual and is a major cause of error in the ISC location method. In certain cases, however, the residual can be used to more accurately locate an earthquake as it is, in effect, an estimation of the earth's lateral inhomogeneities along the path between a specific source-receiver pair (Everenden, 1969).

The approach used is called the master event relocation method. In this study, it is used to relocate the events of the foreshock/aftershock sequence. The largest magnitude event of a sequence (referred to as the main shock) is recorded by more seismic stations than other events in the series. It should be the most accurately located event and thus should have the most accurately calculated travel-time residuals. Since the events of a single series occur within a relatively small area, the travel path for a seismic ray between any of the events and a specific receiver is assumed to be the same. The residuals calculated from the main event for specific source-receiver pairs are then removed from the travel time

for the same source-receiver pair of the smaller events. This in effect removes the lateral inhomogeneities of the earth and gives better relative location. Mapping of relocated epicenters in both cases in this study improved the accuracy in choosing the fault plane.

GEOLOGY

Most of Alaska and Chukotka are geologically complex. Much of the area is a collection of different tectonstratigraphic terrains (Jones et al., 1977, 1981; Jones and Silberling, 1979; Berg et al., 1978; Churkin et al., 1979, 1980; Fujita and Newberry, 1982, 1983). Alaskan studies are further complicated by areas of large-scale thrust faulting (Sainsbury, 1969) and strike-slip faults (Grantz, 1966). These areas and their structural features are located on Figure 3. The following is a geological and structural summary of the study area:

Seward Peninsula

The Seward Peninsula is dominated both by Precambrian gneiss and sediments, with the remainder being composed primarily of Mississippian carbonates and limestones (Sainsbury et al., 1970; Hudson, 1977). The geologic map of Seward Peninsula compiled by Hudson (1977) shows that the southern and western portions are heavily faulted. Large-scale thrust faulting was first inferred by Collier (1902). It has since been shown that thrust sheets occur over most of the peninsula (Sainsbury, 1969; Sainsbury et al., 1970). Sainsbury et al. (1970) show that thrusting probably occurred in the Early Cretaceous. Two large normal faults with signs of recent activity are observed in the southern part of the peninsula (Nakamura et al., 1980). The faults both trend east-west and lie along the Bendeleben and Kigluaik Mountains.

FIGURE 3

INDEX MAP OF THE STUDY AREA

The areas marked by vertical lines are ophiolites described by Patton et al., (1977). The dotted line is the boundary between uplifts (south) and depressions (north). The intraplate earthquakes studied are located on the map. The number by each earthquake refers to TABLE 1.

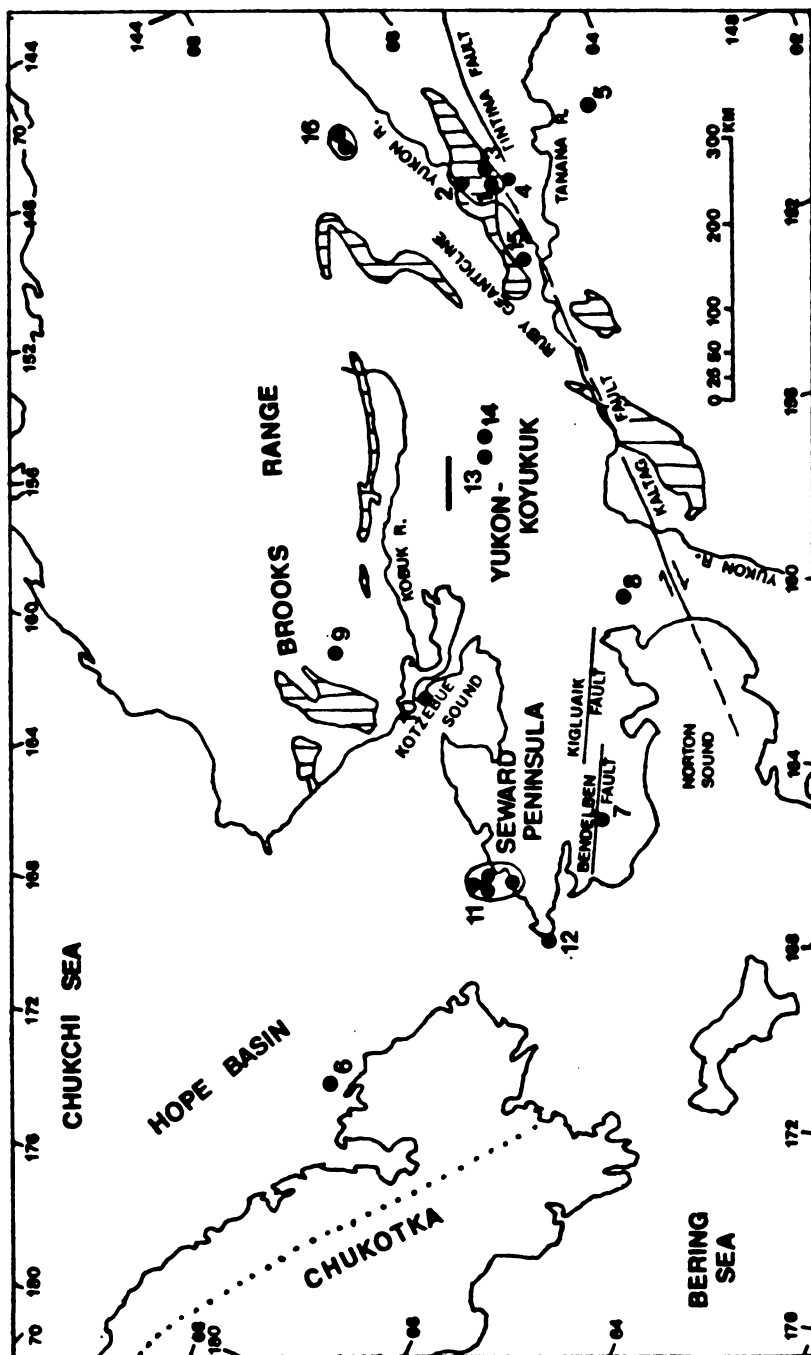


FIGURE 3

Western Brooks Range

The Western Brooks Range is primarily composed of Paleozoic carbonates, sandstones, and conglomerates which are intruded by Devonian granitoid plutons (Beikman, 1980). A series of rootless ophiolites emplaced during the Middle Jurassic to Early Cretaceous have been mapped by Patton et al. (1977). Dating by the K-Ar method has yielded Jurassic ages for the ultramafic layered gabbro complex (Patton et al., 1977). The compressional forces which emplaced the ophiolites also caused thrusting within the Western Brooks Range. The area was shortened by at least 100 km (Martin, 1970) with a maximum possibly in excess of 250 km (Snelson and TAILLEUR, 1968).

Yukon-Koyukuk Province

The Yukon-Koyukuk province is a wedge-shaped region in the center of the study area. The province is composed of a central volcanic pile of Cretaceous age with a huge thickness of volcanically derived sediments flanking the central pile on all sides (Patton, 1973). The volcanic sediments may be as thick as 25,000 feet (Patton, 1973). Jurassic ophiolites border the province on the north and southwest margins (Patton, et al., 1977). These slab-like bodies dip beneath the volcanic sediments at angles between 10 and 80 degrees and have been interpreted as the root zone for ophiolites in the Western Brooks Range and Ruby Geanticline (Patton et al., 1977). The province is offset on the south end by the Kaltag fault, a right-lateral strike-slip fault (Patton, 1973; Patton et al., 1977). Displacement as determined by offsets of alluvium, is from 65 to 130 km (Patton and Hoare, 1968). Three smaller faults of unknown type with general northeast-southwest trends have been mapped in

the central and northeast portions of the province (Patton and Hoare, 1968).

Ruby Geanticline

The Ruby geanticline is a northeast-southwest striking Cretaceous uplift approximately 350 km long and 100 km wide. The central portion of the uplift is composed of Precambrian and Paleozoic schist and quartzite and is intruded by granites of Lower Cretaceous age (Miller et al., 1959). A discontinuous belt of ophiolites of Jurassic to Triassic age occur along the southeastern side of the uplift. Patton et al. (1977) believe this belt to be the remnant of an ophiolite sheet, once continuous, that covered the Ruby geanticline. The root zone of that ophiolite sheet became the present, narrow discontinuous belt of ophiolites observed along the southeastern border of the Yukon-Koyukok province. The Kaltag fault has offset the southeastern portions of both the metasedimentary rock and the ophiolite belt from 80 to 130 km (Patton et al., 1977).

Central Alaska

The Yukon and Tanana rivers border a geologically and structurally complex area in central Alaska. The region is composed of six tectonostratigraphic terrains which all have general northeast-southwest trends (Jones et al., 1981). The terrains are primarily fault bounded (Beikman, 1980). From northwest to southeast they are the Innoko, Wickersham, Livengood, White Mountain, Minchumina and Yukon-Tanana (Jones et al., 1981). For descriptions of the individual terrains see Jones et al. (1981).

Chukotka

Chukotka is the northeastern most portion of Siberia. Structurally it is composed of a region of slight (500m to 700m) Pliocene to Quaternary uplifts in the central and southern portions and a band of Pliocene to Quaternary depressions on the northern margin (Goryachev et al., 1968). The boundary between the two regions has a northwest-southeast trend and is shown in Figure 3. Two small exposures of ophiolites with probable Jurassic emplacement ages, have been identified in the region (Fujita and Newberry, 1982). It has been suggested that the same tectonic event emplaced both the Chukotka and central Alaska ophiolites (Fujita and Newberry, 1982). Precambrian rocks outcrop on the eastern end of the peninsula while Carboniferous rocks are predominant on the northern shore.

Southern Hope Basin

North of Chukotka is a sedimentary prism deposited in the Hope Basin. Using velocity studies gathered from seismic reflection data, Grantz et al. (1975) conclude that deformed Paleozoic metamorphics underlie the southern portion of the basin. The basin's structural axis parallels the coastline of northern Chukotka (Grantz et al., 1975). It appears to have formed by crustal extension due to the east-northeast movement of northern Alaska along the Kaltag fault in early Tertiary times (Patton and Hoare, 1968; Grantz et al., 1975).

SEISMICITY

Figure 1 is a map of epicentral locations for all earthquakes that have occurred in the study area since 1900. Most of the events are confined to one of the numerous seismic regions, defined here as areas exhibiting higher levels of seismicity than surrounding areas. Most of the seismicity is of low magnitude with only a few earthquakes which have body wave magnitudes greater than 5.0. The following is a description of the seismic regions in the study area. All magnitudes stated within the text are body wave magnitudes unless otherwise noted. Specific earthquakes will be referenced as to the year-month-day and (where need be) hour.minute.second of occurrence.

Seward Peninsula

The Seward Peninsula is an area of apparently low seismicity. Events with sufficient magnitude to be recorded teleseismically are confined to the southern half of the peninsula. The largest of these events, a magnitude 5.3 shock, occurred on 64-12-13 in the Kigluaik Mountains and had epicentral coordinates of 64.96N, 165.4W. It appears that much of the seismic activity on Seward Peninsula is undetected by seismic stations around the world due to the low magnitudes of most events. A local seismograph network installed by the NOAA recorded about 300 earthquakes with magnitudes (M_L) between 1.0 and 4.5 over a two year period (1977-1978). A plot of these epicentral locations by Biswas et al. (1980) is

shown in Figure 4A. Biswas et al. (1980) suggest that most of the epicenters occur in linear trends which can be related to the structural features and fault zones of Seward Peninsula and the surrounding area such as the Kigluaik Mountains and the Kaltag fault (Figure 4B).

Yukon-Koyukuk Province

The Yukon-Koyukuk province exhibits three zones of seismicity. The center of the smaller, less seismically active zone is located at 64.6N, 160.2W in thick Cretaceous sediments. A magnitude 5.8 event occurred within this zone on 65-4-16 and has been studied by Sykes and Sbar (1974) and Liu and Kanamori (1980). It is interesting to note that this event, like the Kigluaik event on Seward Peninsula, had no foreshocks or aftershocks associated with it as do many of the larger intraplate earthquakes of Alaska.

In the large Cretaceous volcanic pile located in the northcentral portion of the Yukon-Koyukuk province at 66N, 156.6W is a seismic zone of much greater extent with larger-magnitude earthquakes, and more numerous, smaller events. The Huslia series occurred within this zone. This series consisted of a main shock (on 58-4-7 at 15.30.40) of Gutenberg-Richter (G-R) magnitude 7.3 and a one week long aftershock series (Davis, 1960). Two of the aftershocks had G-R magnitudes of 6.5 and were recorded teleseismically.

The third zone is a north-south trending band of epicenters located between 66.0N and 66.5N at 157.5W. All of the events in this area have low magnitudes (less than 4.0) and many occur as earthquake pairs.

FIGURE 4.

SEISMICITY OF WESTERN ALASKA

The data was gathered by a local seismograph network operated by the National Oceanic and Atmospheric Administration during 1977-78 and were mapped by Biswas et al. (1980).

4A - Epicentral locations

4B - Relation of earthquakes to structural features

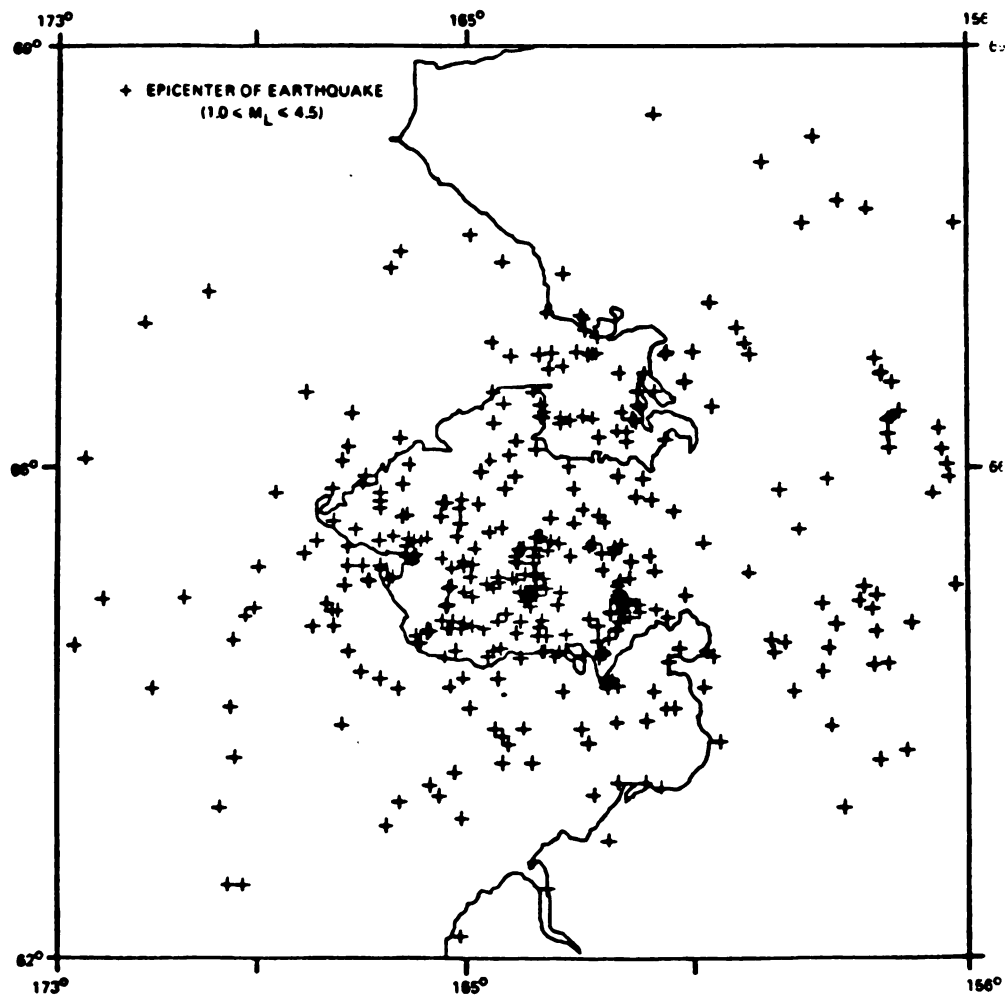


FIGURE 4A

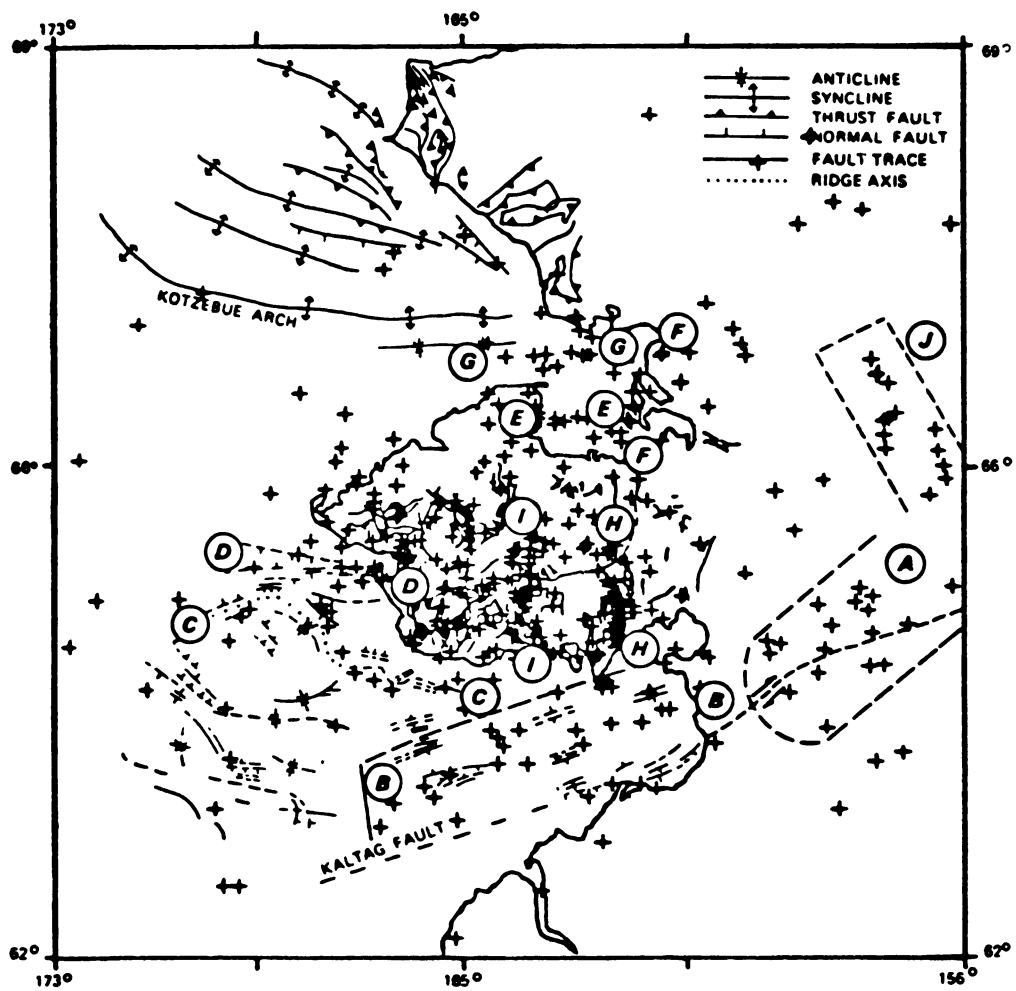


FIGURE 4B

Western Brooks Range

The western Brooks Range has many widely scattered, lower magnitude earthquakes. The only area of high epicentral density occurs at 67.8N, 161.5W. Almost all of these events are part of the foreshock and aftershock sequence of the 81-7-12 event which had a magnitude of 5.2. The sequence occurred between 81-7-4 and 81-8-3 and consisted of 17 events.

Central Alaska

The density of earthquakes in the central Alaska area is similar to the Huslia seismic zone of the Yukon-Koyukuk province except for the prominent north-south alignment of epicenters stretching from 65.0N to 66.0N at longitude 150.0W. Most of the events within this cluster were part of the Rampart sequence of 1968. A magnitude 6.0 earthquake occurred on 68-10-29 at 22.16.16 and was followed by at least 140 aftershocks which occurred over a three month period. Other events and smaller sequences have occurred along the same fault zone but none with as great a magnitude or aftershock duration as the 1968 Rampart sequence.

Two other areas in central Alaska have experienced earthquakes of larger magnitudes than most of the area's events. Two earthquakes, both of G-R magnitudes 6.3 with epicenters at 65.2N, 152.0W occurred on 58-5-10 and 58-5-11. No related foreshock or aftershock sequence was recorded, possibly due to the poor seismograph station coverage in the 1950's. It should also be noted that these events occurred about one month after the main shock of the Huslia sequence.

In another series, two earthquakes with epicenters located at 66.8N, 148.2W occurred on 66-12-20. The magnitudes were 4.8 and 4.9. No foreshock or aftershock sequence was recorded.

Chukotka and Southern Hope Basin

Seismic activity in this area is centered at 68.0N, 173.0W. Three of the events occurred as a series in February of 1928, the largest being of G-R magnitude 6.9. Recent seismicity in the area includes two magnitude 5.0 earthquakes, one in 1962 and the other in 1971. Other than this seismic region, there are very few teleseismically located events.

A map including very low magnitude earthquakes (as low as 1.0 unified USSR magnitude) compiled from the Akademiya Nauk SSSR "Novi Katalog Sil' nikh Zemletryasenii SSSR" (Kondorskaya and Shebalin, 1977) is shown in Figure 5. This area, like the Seward Peninsula, exhibits a high level of low magnitude earthquakes. A north-south trending zone of epicenters occurs at 178.5W but is probably a bias due to the location technique. The seismicity is more active in the northern portions of this region than in the southern. It is interesting to note that the border between the northern and southern zones falls on what Goryachev et al. (1968) have mapped as the border between "considerable Pliocene-Quaternary uplift" to the south and "Pliocene-Quaternary depressions" to the north. Earthquakes which are of such low magnitudes that they can only be recorded by local seismograph networks may occur with more frequency than is presently believed. The magnitude 5.0 event of 71-10-5 is reported in the ISC Bulletin as a single event. However, Lazareva (1970) reports an associated aftershock sequence of 50 events which were recorded by a local station.

Areas of No Seismicity

As the previous sections have pointed out (particularly the Seward Peninsula section and Chukotka and Southern Hope Basin portion), many

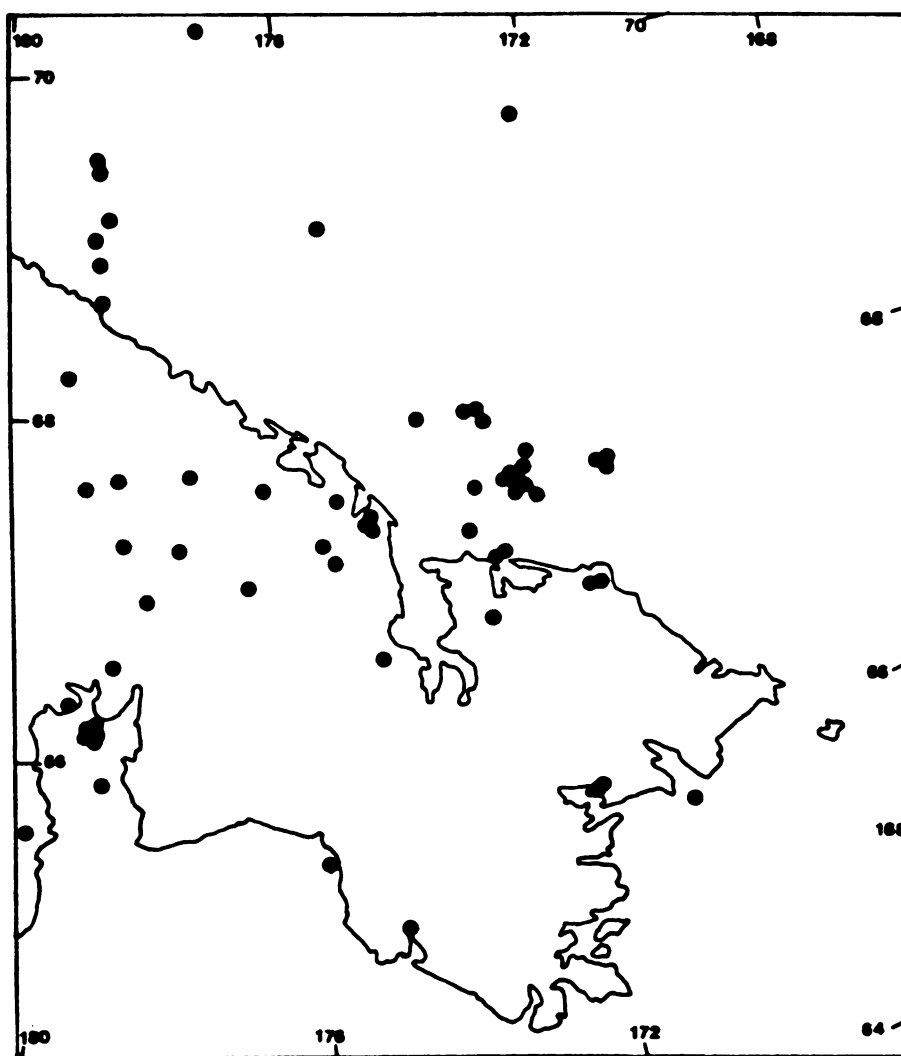


FIGURE 5
CHUKOTKA EPICENTERS

of the areas which appear as aseismic regions in Figure 1 actually exhibit high levels of lower magnitude seismicity. Examples are northwestern Chukotka, Norton Sound, northern Seward Peninsula and the western Yukon-Koyukuk province. This still leaves large areas covered by oceans and much of northern Alaska as being aseismic with respect to teleseismic events. Whether local seismograph networks in these regions would reveal an abundance of low magnitude seismicity as it did on Seward Peninsula or that they may be truly aseismic areas remains to be seen.

FOCAL MECHANISMS

Focal mechanisms for twelve earthquakes are constrained in this study. Four additional mechanisms were obtained from previously published data. The following is a discussion of the methods used to constrain each focal mechanism. The event number listed in the title of each section and referenced within the text refer to Table 1.

Rampart Series (Event 1)

The main event of the Rampart series occurred on 68-10-29 at 22.16.16 and has an epicentral location of 65.46N, 150.07W. It was a magnitude 6.0 earthquake and is the most widely recorded event in the study area with 312 reported arrival times in the ISC Bulletin. Accompanying the main event was a long and active aftershock sequence which lasted for approximately three months and consisted of 140 earthquakes, the largest of which occurred on 68-10-31 at 00.25.46 and had a magnitude of 4.6.

First motion data was read from WWSSN and Canadian Network records when possible and was supplemented with first motions reported in the ISC Bulletin. Figure 6 is a plot of the first motion data and shows the nodal planes which best fit the data.

For the main Rampart event, the Rayleigh wave amplitude from 14 seismic stations were calculated for four different frequency intervals centered at 40 sec., 50 sec., 60 sec., and 70 sec. All of the plots exhibit similar four-lobed patterns with the pattern orientation varying

FIGURE 6

FIRST MOTION DATA OF EVENT 1.

First motion data for all earthquake focal mechanisms in this study are plotted on a lower hemisphere stereographic projection and are reported as follows:

- - Compression read from short and long period seismic record
- - Dilatation read from short and long period seismic record
- - Compression read from short period seismic record
- - Dilatation read from short period seismic record
- - Compression reported in the International Seismological Summary (ISS) or the International Seismological Center (ISC) Bulletin
- - Dilatation reported in the ISS or ISC Bulletin

The fault plane, when known, is marked by a double slash (/ /). Fault planes marked with dashed lines are poorly constrained. Shaded or cross-hatched quadrants are compressional.

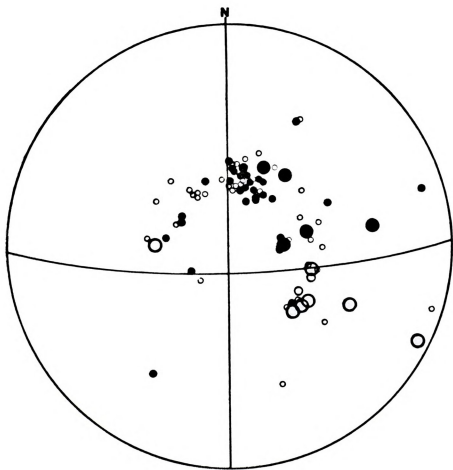
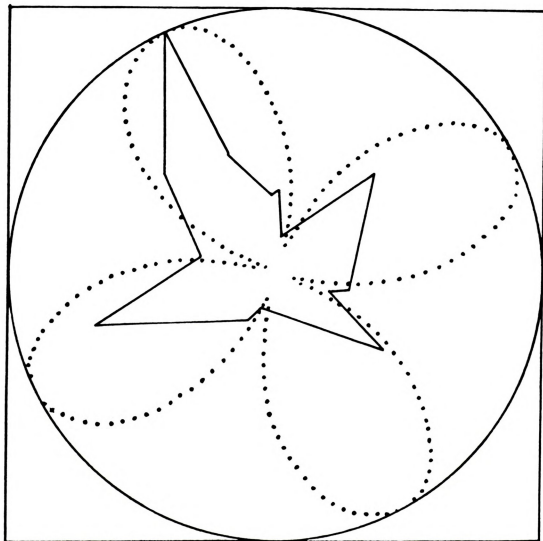


FIGURE 6

less than 10 degrees. Figure 7 shows the pattern calculated from the data (solid line) for a 60 sec. band. The best fit theoretical pattern is given as the dotted line. Gedney (1970) used first motion data read from Canadian, Alaskan, and WWSS network records and obtained nodal planes with similar strikes and dips to those determined in the Rayleigh wave study. Gedney's data are shown in Figure 8.

The fault was constrained by a study of the aftershock sequence. Epicenters reported in the ISC Bulletin for the sequence are shown in Figure 9A and exhibit a general trend of N12E. The master event relocation program of K. Fujita was used to obtain a more accurate epicentral trend. Relocated epicenters are plotted in Figure 9B. The relocated epicentral trend is now N8E. The larger dots in Figure 9B correspond to earthquakes in which more than 20 stations were used in relocation, which should yield more accurate locations than events using fewer stations. These also exhibit the N8E trend. Gedney (1970) noted that the Minook Creek Valley, a linear topographic feature with a N8E trend, lies within the epicentral zone and is probably the surface expression of the fault plane for the Rampart series (see Figure 9A). Although the relocation places the aftershock epicenters about five km to the west of the Minook Creek Valley, the similarities of the trend still suggest that the valley is the fault's surface expression. It is also possible that a slight westerly bias exists in the relocated epicenters.

The first motion and Rayleigh wave focal mechanisms are similar in that both are consistent with strike-slip faults and steeply dipping nodal planes. However, the nodal plane orientations differ by about 20 degrees. A study by Chung and Kanamori (1978) found this same discrepancy in the focal mechanism determination of the New Hebrides earthquake of



STRIKE=200 DIP=80 SLIP=4 PERIOD=60 SEC.

FIGURE 7

RAYLEIGH WAVE RADIATION PATTERN OF EVENT 1

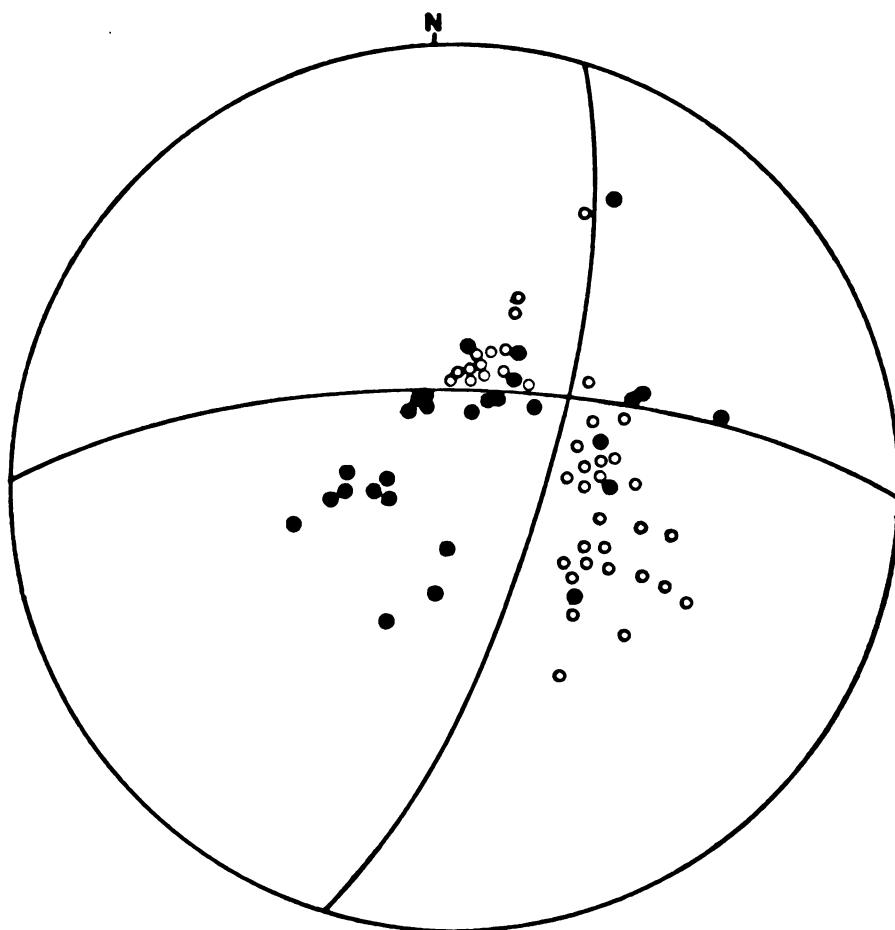


FIGURE 8
GEDNEY (1970) DATA FOR EVENT 1

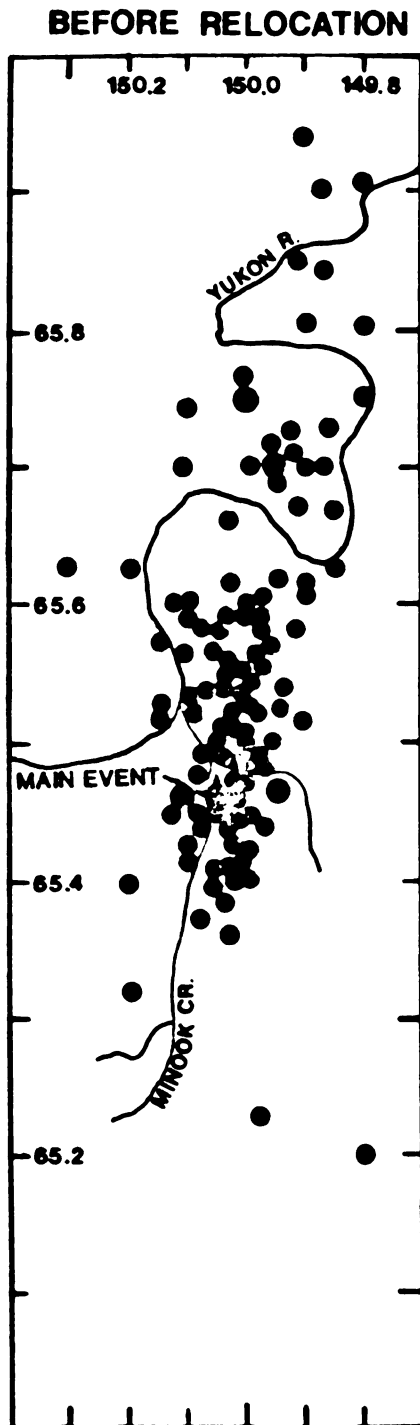


FIGURE 9A

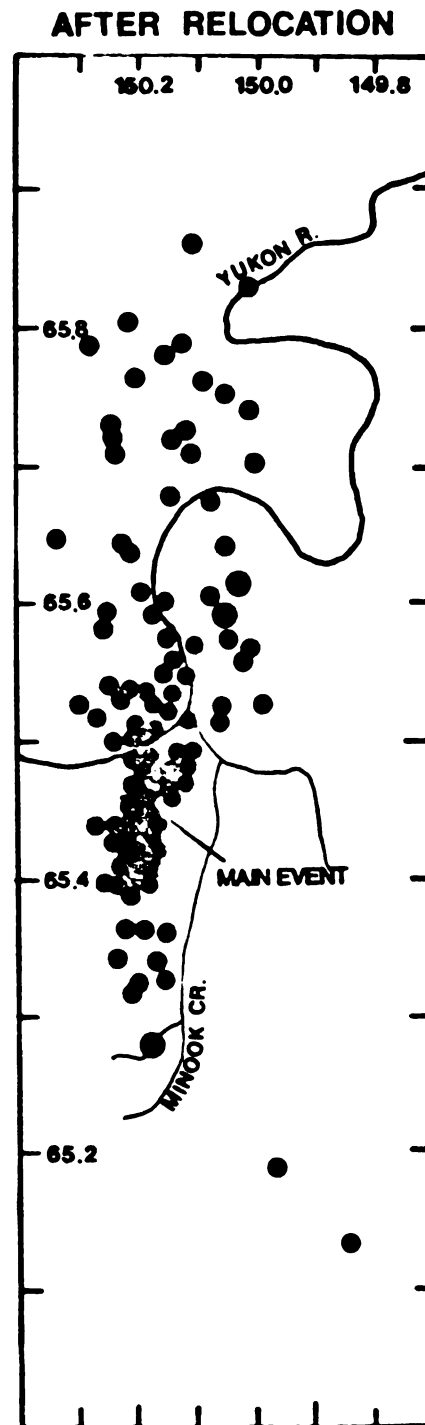


FIGURE 9B

AFTERSHOCK RELOCATION FOR EVENT 1

January 19, 1969. They suggested that since the two mechanisms are constructed from different portions of the seismic signal, that it is not unusual for the focal mechanisms to differ slightly. They went on to suggest that in the case of a complex rupture along the fault, the seismic signature of the Rayleigh wave may be complicated by seismic energies from other ruptures. It is likely that the main Rampart event, which was associated with a very active aftershock sequence, was not a simple, single rupture event. The final mechanism, shown in Figure 10, chooses nodal plane orientations which agree with the observed fault trend and lie between the nodal planes of the two focal mechanisms.

Event 2 is one of the larger aftershocks in the Rampart series. It occurred on 68-11-3 at 7.37.39 at location 65.47N, 149.86W and had a magnitude of 4.4. First motion data read from WWSSN records and those reported in the ISC Bulletin were used in an attempt to determine the focal mechanism (Figure 11). Although there are not enough data for accurate determination of the planes, the data that are available show a mechanism similar to that of the main Rampart event is not possible. There is a much larger component of either normal or reverse faulting and the nodal plane orientation must be different from the main event. Other earthquakes which have occurred within the area of the Rampart aftershock zone (though not within the 1968 Rampart series itself) also have focal mechanisms different than the 1968 event. Bhattacharya and Biswas (1973) used local seismic network records to determine the mechanism for event 3 which occurred less than 10 km from the main Rampart event. The mechanism is shown in Figure 12. It is a very well constrained mechanism and is that of a normal fault with a horizontal B-axis. Event 4 is an earthquake which occurred on 61-01-30 near the southern end of the aftershock

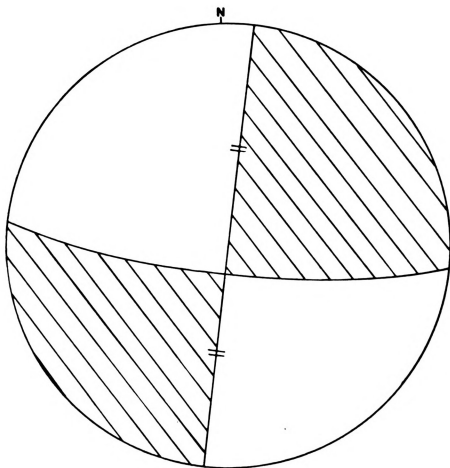


FIGURE 10
FINAL MECHANISM FOR EVENT 1

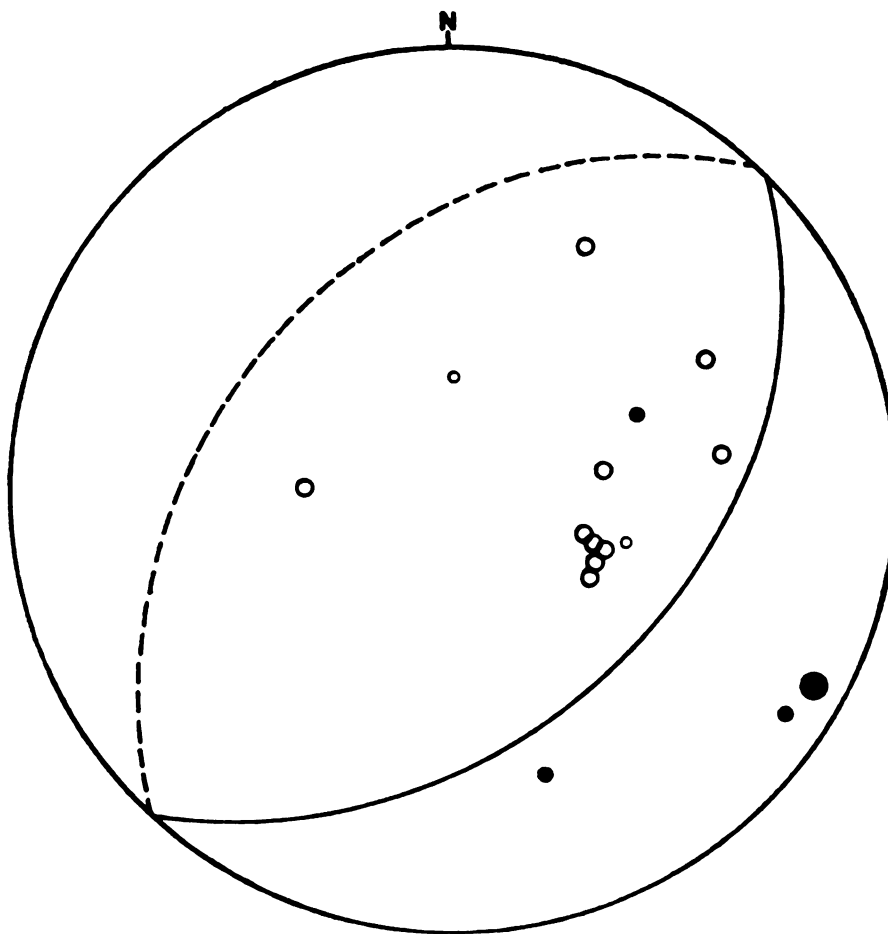


FIGURE 11
FIRST MOTION DATA FOR EVENT 2

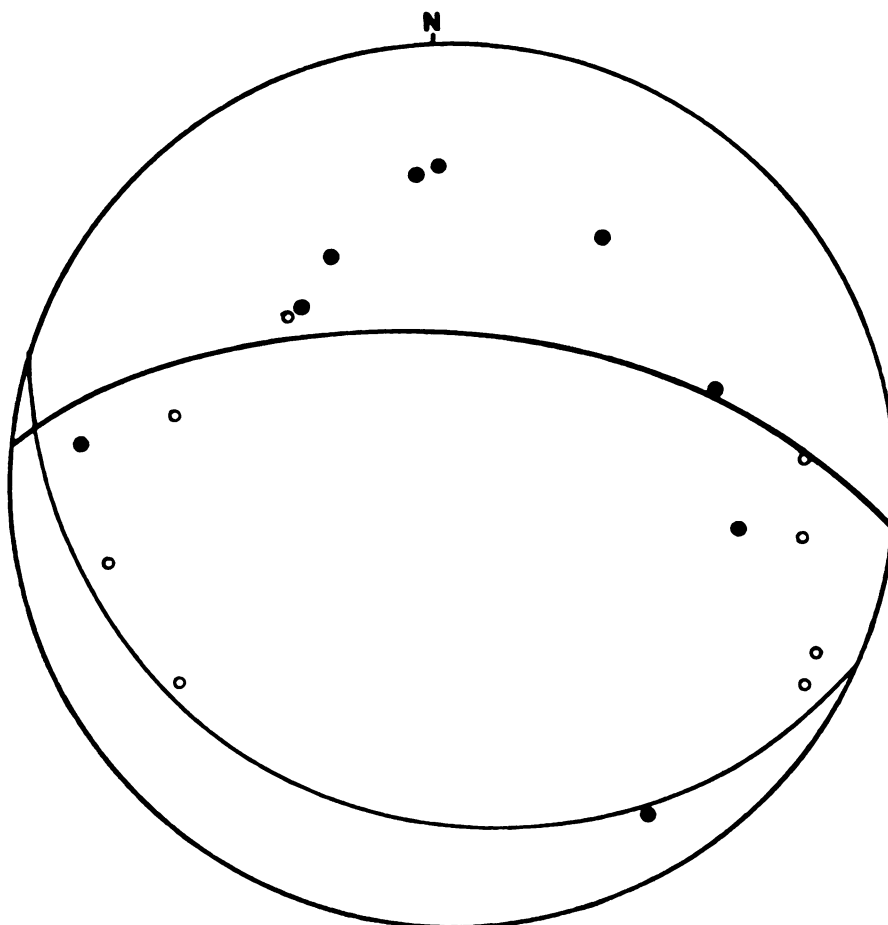


FIGURE 12

FIRST MOTION DATA FOR EVENT 3
Data are from Bhattacharya and Biswas (1979).

zone at 65.2N, 150.2W. The first motion data from the ISS are plotted in Figure 13. Though only eleven first motions were reported, they are sufficient to show that the mechanism has a much larger component of reverse faulting than the main Rampart event. Gedney (1970) used local seismic network data to determine the mechanism for event 5. It is a magnitude 5.4 earthquake with an epicentral location to the south of the 1968 Rampart series at 64.8N, 147.4W. A strike-slip mechanism similar to the main Rampart event was obtained and is shown in Figure 14.

In order to obtain such a diverse group of focal mechanisms, a complex tectonic scheme is necessary. There are many factors which could affect the stress regime in the Rampart zone as shown in Figure 15. First, the Kaltag-Tintina and McKinley-Denali fault systems, both long strike-slip faults, are part of a system of large strike-slip faults which bisect the southern portion of Alaska (Grantz, 1966). The Kaltag-Tintina system passes through the Rampart area. Second, there is a bend in both of these fault systems which lies about 130 km to the east of the Rampart area. It has been suggested that the bend may have formed when Arctic Alaska rotated from the Canadian Arctic to its present position (Freeland and Dietz, 1977) and could have an effect on the local stress orientation. Finally, there is the stress applied by the subducting lithosphere to the overriding continental plate. Even though the subduction zone is located 400 km to the south, VanWormer et al. (1974) have mapped the top of the lithosphere beneath south central Alaska and found that it is at a depth of 50 km at a point 175 km south of the Rampart zone. At such a shallow depth it is probably coupled to the continental crust and thus would effect the stress regime.

Another suggestion for the diverse focal mechanisms seen in the

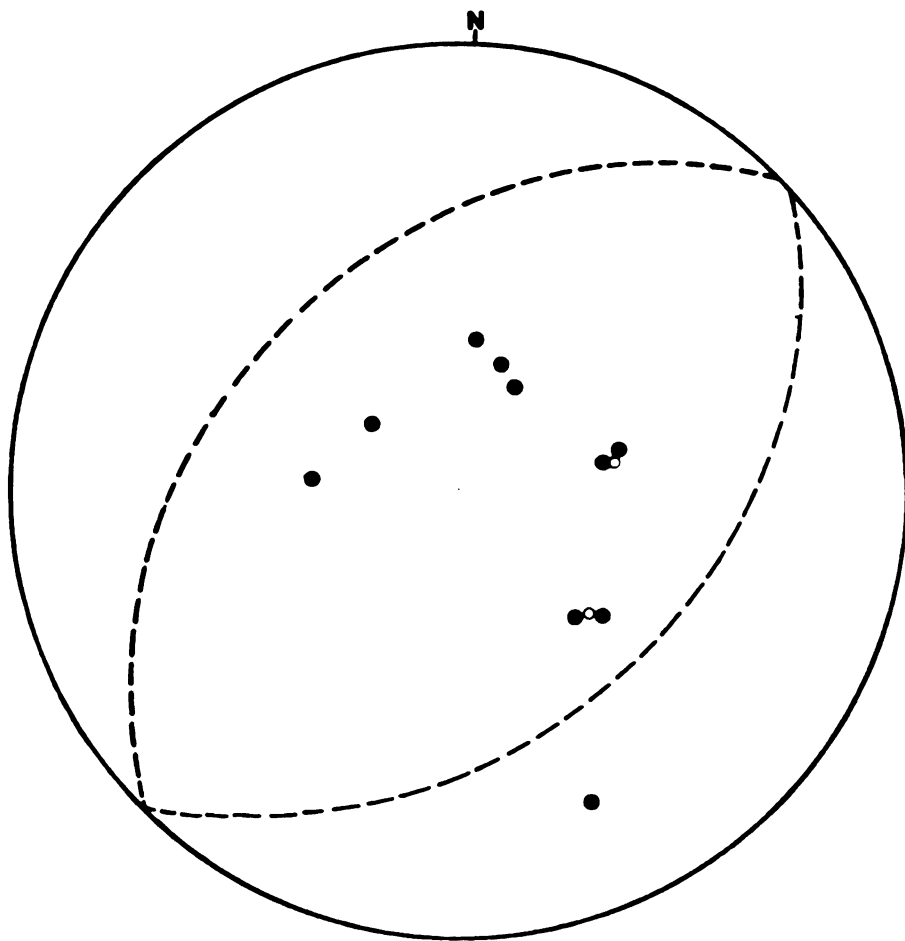


FIGURE 13
FIRST MOTION DATA FOR EVENT 4

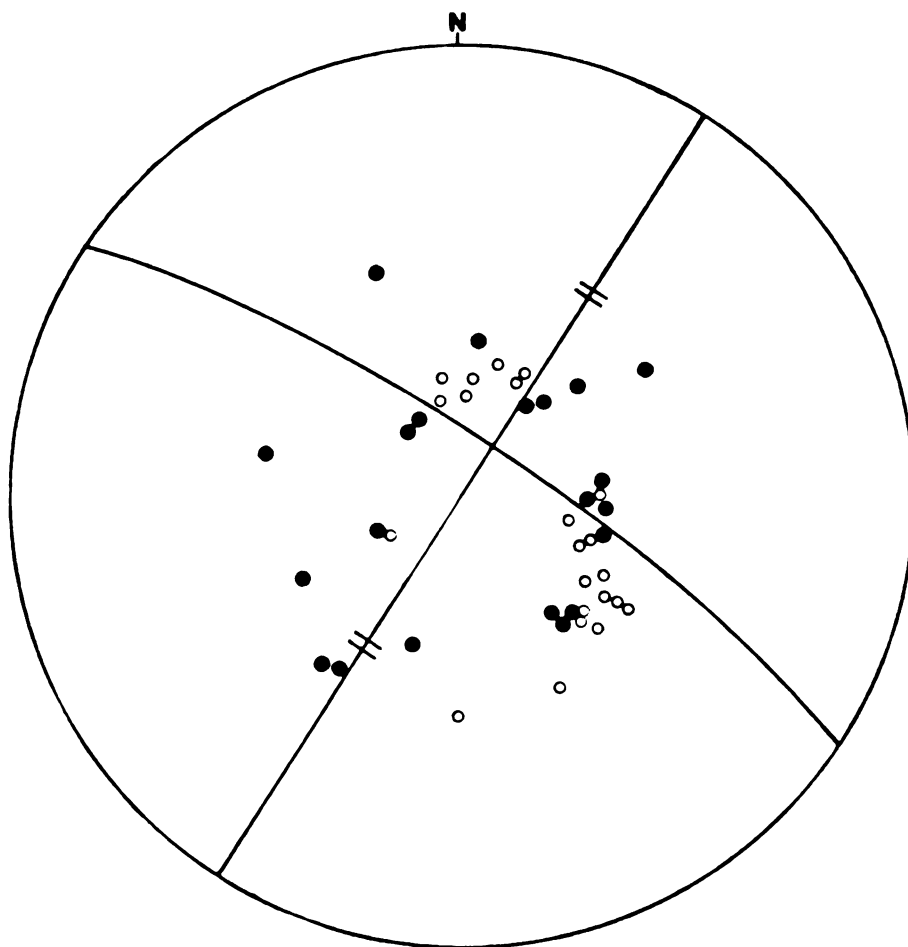


FIGURE 14

FIRST MOTION DATA FOR EVENT 5
Data are from Gedney (1970).

FIGURE 15

STRUCTURAL FEATURES NEAR THE RAMPART SERIES

The faults are dashed where inferred. The lines in the lower left are depths to the top of the subducting oceanic crust as determined by VanWormer et al. (1974). The box surrounds the Rampart aftershock zone.

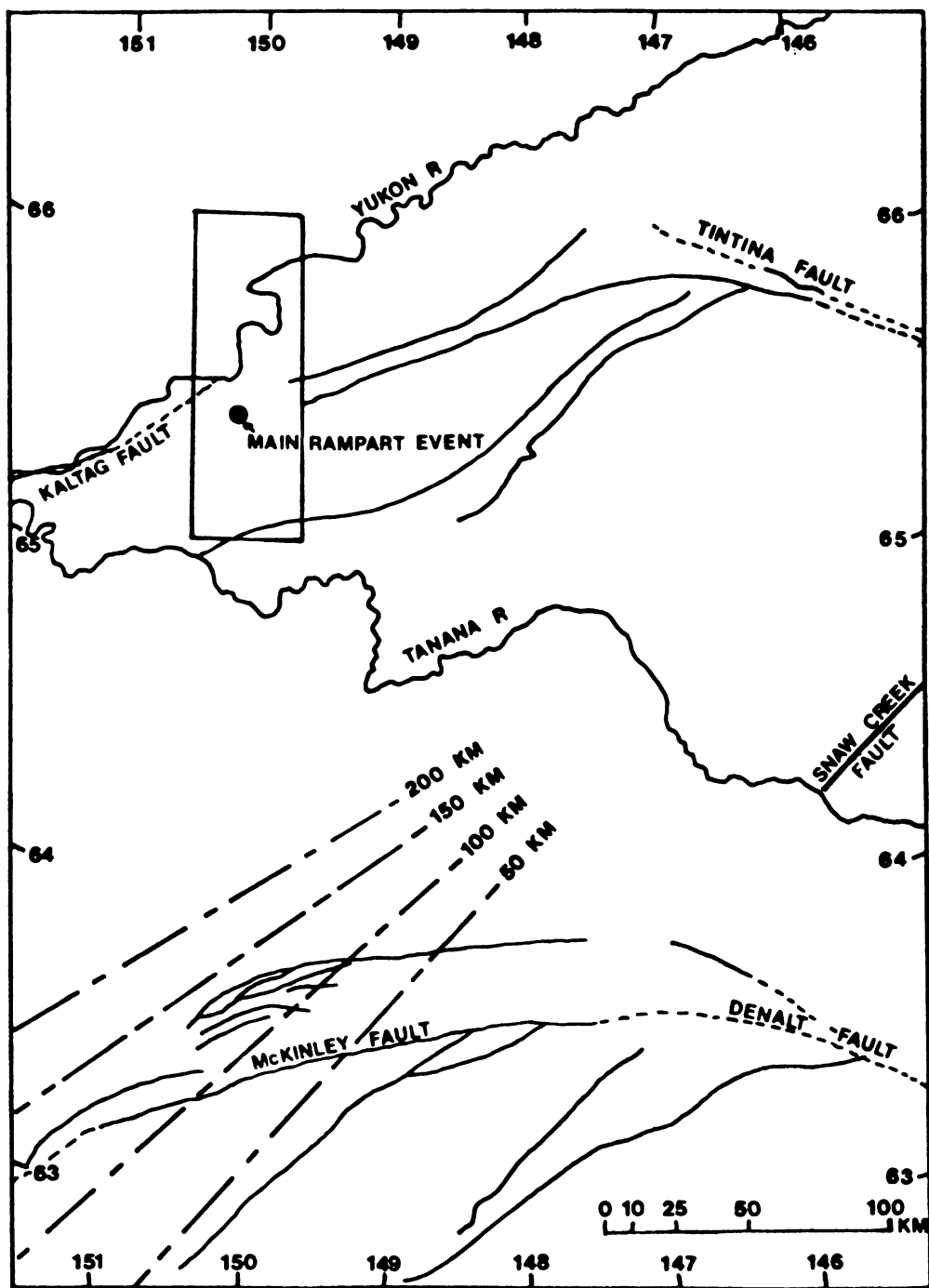


FIGURE 15

Rampart zone is based on a model by Weaver and Hill (1978/79) for earthquake swarms in California. In their study they note that earthquake swarms with normal fault mechanisms which may be associated with small crustal spreading centers tend to be located between pairs of strike-slip faults. Their model is shown in Figure 16. Gedney et al. (1980) suggest that a seismic zone near Fairbanks, Alaska, about 150 km to the southeast of the Rampart zone, may be similar to the Weaver and Hill (1978/79) zone. Although this model cannot explain all of the anomalous events, striking similarities exist between the Rampart and California zones such as the large strike-slip faults, the normal and strike-slip focal mechanisms and the fault orientations.

Chukotka Earthquake (Event 6)

The Chukotka earthquake occurred on 71-10-5 and has epicentral coordinates of 67.38N, 172.57W. It was a magnitude 5.2 event and was recorded by 133 seismic stations. There was no associated foreshock or aftershock sequence reported in the ISC Bulletin. It is the only event in Chukotka or southern Hope Basin of sufficient magnitude to enable a focal mechanism solution.

The Rayleigh wave radiation pattern was calculated for seismic waves with mean periods of 30 sec., 40 sec., 50 sec., and 60 sec. Data for the 50 sec. period wave are shown in Figure 17. In all, records from 23 stations were used. The spectral amplitudes for each station's record were examined. Records which exhibited many spurious amplitude peaks were not used in the final Rayleigh wave radiation pattern. This technique allowed for the elimination of seven stations. The pattern after station deletion is shown in Figure 18. Comparison with Figure 17 reveals little

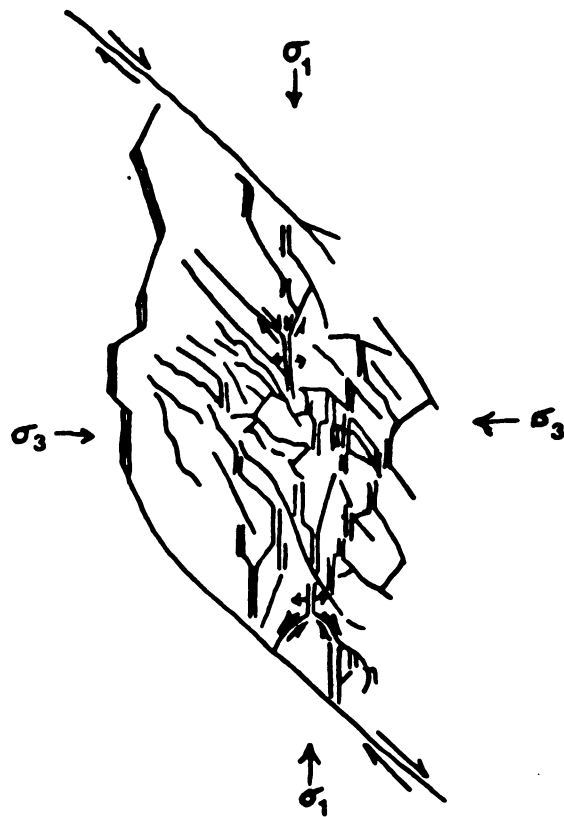
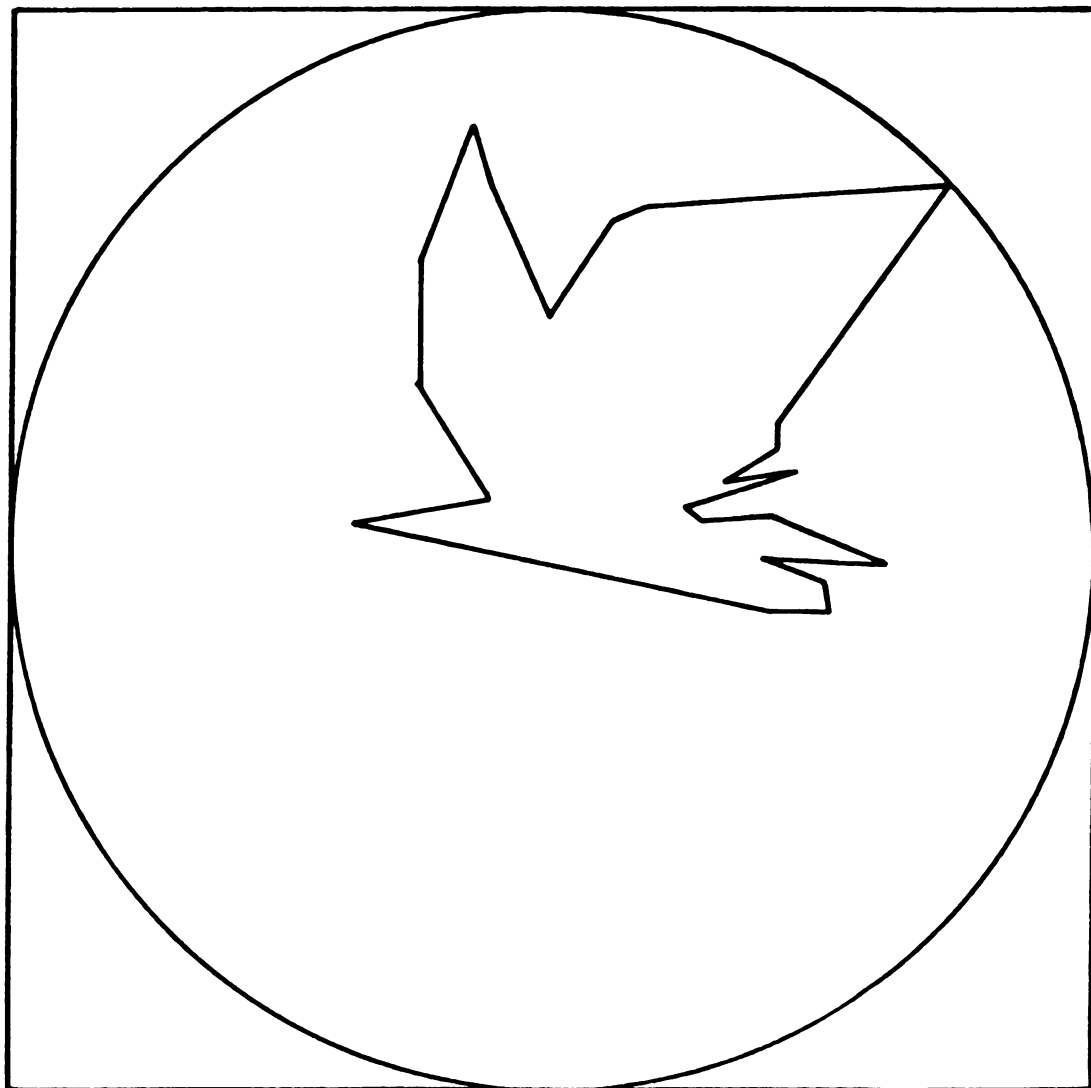


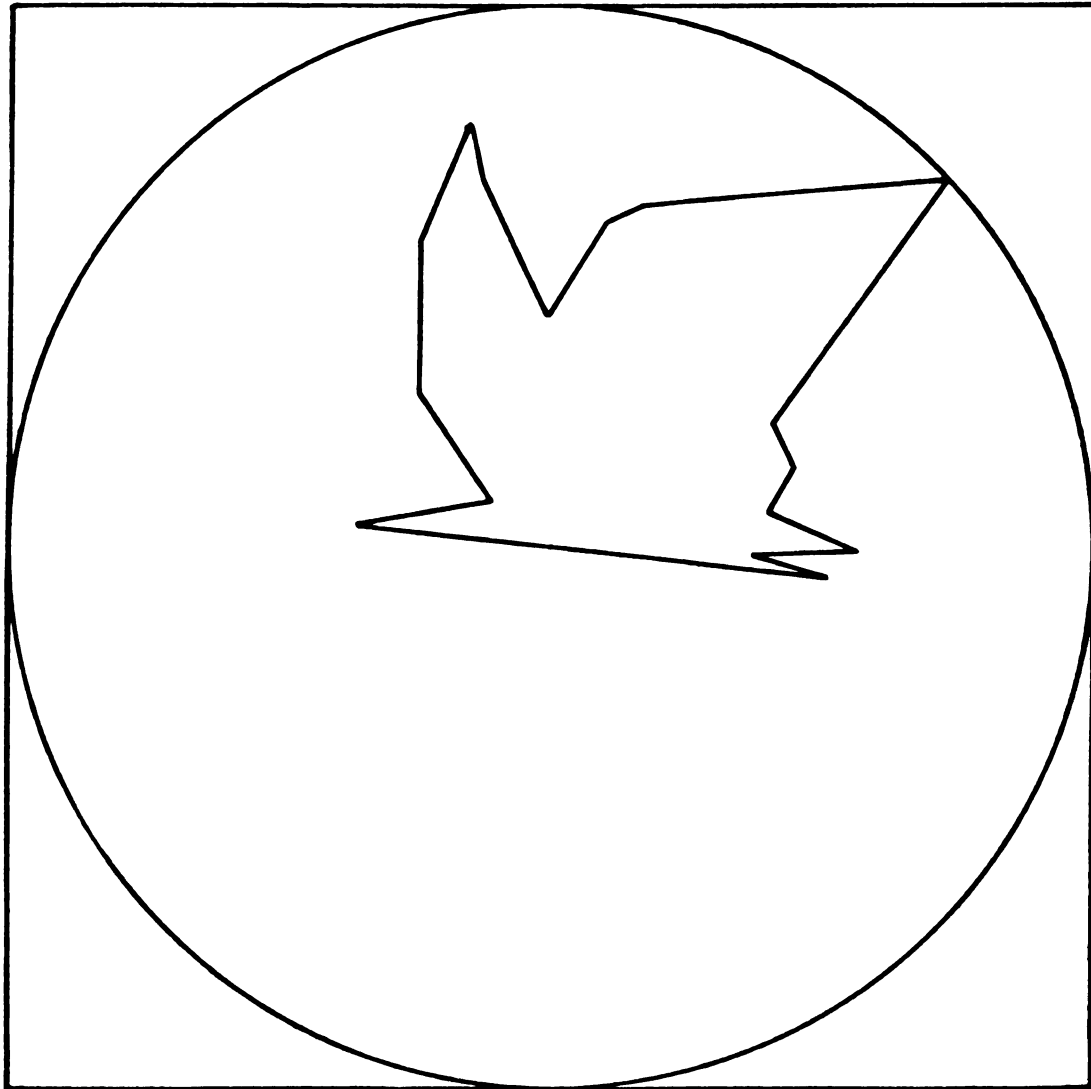
FIGURE 16
MODEL OF WEAVER AND HILL (1978/79)



PERIOD = 50 SEC.

FIGURE 17

RAYLEIGH WAVE RADIATION PATTERN OF EVENT 6 BEFORE STATION DELETION



PERIOD = 50 SEC.

FIGURE 18

RAYLEIGH WAVE RADIATION PATTERN OF EVENT 6 AFTER STATION DELETION

change in the pattern before and after station deletion.

The Rayleigh wave radiation pattern offers few constraints, if any, on the focal mechanism. If data from stations with azimuths between 110 and 270 degrees was available, better definition of the pattern lobes may have been possible. Another problem may be that the earthquake was not of sufficient magnitude to enable the recording of the surface waves at large distances. The seismic signal was low in magnitude, often just above background noise. In any event, the Rayleigh wave data is inconclusive.

First motion data read from WWSSN records and Canadian Network records and reported in the ISC Bulletin are plotted in Figure 19. The strike-slip mechanism with the nodal planes shown in the figure is the most probable solution and results in only two inconsistent data points. If the compressional pick from station QUE near the B-axis is ignored, a mechanism similar to that in Figure 19 would be very poorly constrained. Such a data set would be better explained by a normal fault mechanism with nodal planes striking approximately east-west. Fujita et al. (1983) suggest this as a possible mechanism for the event. The QUE pick is questionable at best, making the strike-slip mechanism of Figure 19 poorly constrained.

Much of the structural grain in northern Chukotka parallels the N44W trending nodal plane. Voyerodin and Sukhov (1977) note that the trend of the Keukvun'-Iul'tin and Maynypontavaam faults, both "deep seated" faults in northern Chukotka, are N45W. Goryachev et al. (1977) have mapped the boundary of the Pliocene-Quaternary downwarps to the north and the slight Quaternary uplifts to the south as having a trend very close to the N44W trending nodal plane of the focal mechanism. This nodal plane is the

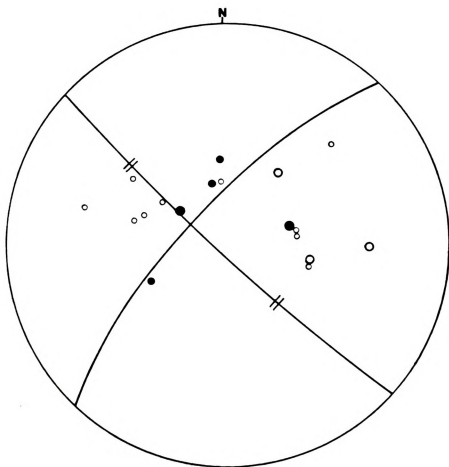


FIGURE 19
FIRST MOTION DATA FOR EVENT 6



probable fault plane.

It should also be noted that the epicenter occurs near the epicenters of four events in 1928 (three of which occurred within one series) of G-R magnitude between 6.2 and 6.9 and a magnitude 5.0 event in 1962. These have been the only large magnitude events in Chukotka and the Hope Basin. All are curiously located within a relatively small area. Fujita et al. (1983) have associated these events with the uplift of Kotzebue arch.

Seward Peninsula (Event 7)

The Seward Peninsula event occurred on 64-12-13 in the southeast portion of the peninsula at 64.88N, 165.75W. It was a magnitude 5.3 event and was recorded by 131 seismic stations. A smaller magnitude 4.5 event preceded the main shock by 1 min. 19 sec. and was the only other event associated with the main shock that was reported in the ISC Bulletin.

First motions were read from WWSSN records and were supplemented by first motion data reported in the ISC Bulletin. The first motions are shown in Figure 20. Although the dilatational first motions outnumber compressions by about 4 to 1, they are distributed such that a focal mechanism cannot be constructed with a high degree of certainty. However, the data in Figure 20 strongly suggest the normal mechanism shown.

The Rayleigh wave radiation pattern was determined for this event and is shown in Figure 21. Twenty nine earthquake records were digitized and used in the original amplitude vs. azimuth plot. To determine the reliability of individual station records, the amplitude spectra were plotted for each of the 29 stations. Using this check, 15 of the 29 stations were discarded. The final plot is seen in Figure 22. The pattern after station deletion is not significantly different than the

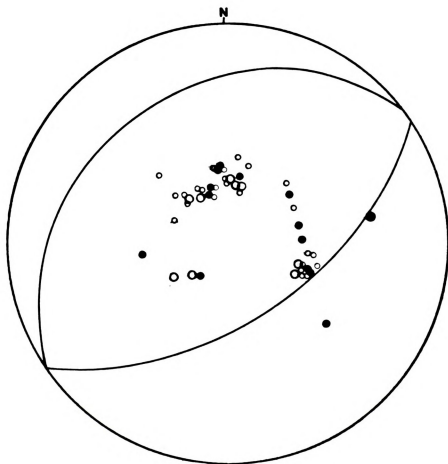
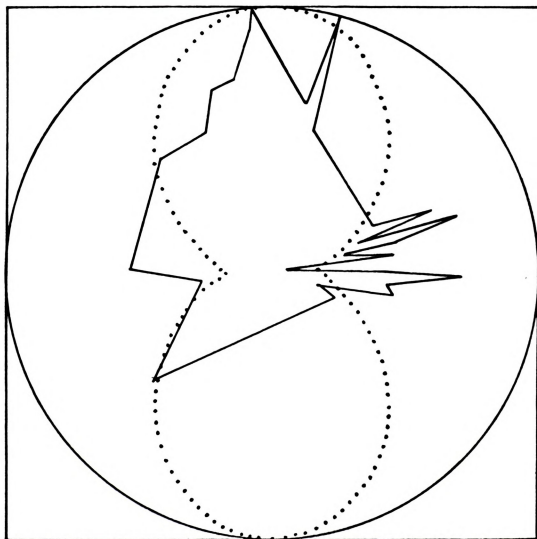


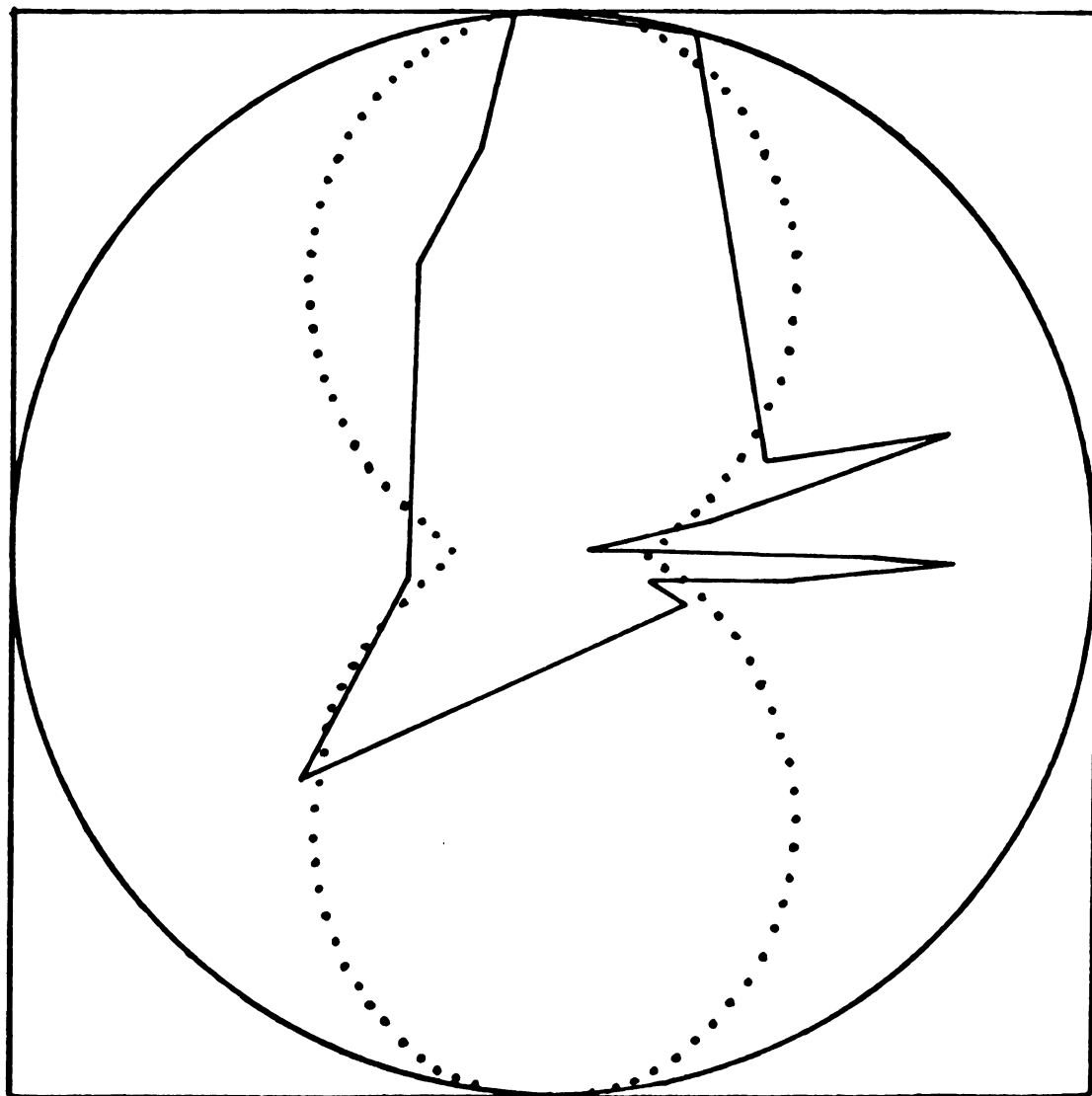
FIGURE 20
FIRST MOTION DATA FOR EVENT 7



STRIKE = 85 DIP = 26 SLIP = 90 PERIOD = 50 SEC.

FIGURE 21

RAYLEIGH WAVE RADIATION PATTERN OF EVENT 7 BEFORE STATION DELETION



STRIKE=85 DIP=26 SLIP=90 PERIOD=50 SEC.

FIGURE 22

RAYLEIGH WAVE RADIATION PATTERN OF EVENT 7 AFTER STATION DELETION

previous pattern. A two lobed pattern is the best fit to the observed data and is not inconsistent with the normal faulting mechanism which the first motions suggest. The computer generated radiation pattern is the dotted line in Figure 22. It is difficult to determine the exact inclination of the B-axis from this radiation pattern though it appears to be within 20 degrees of the horizontal. Thus, the amount of the strike-slip component of motion is not accurately known. If a horizontal B-axis is assumed, the mechanism shown in Figure 20 is obtained.

The focal mechanisms from the first motion data and the Rayleigh wave data both indicate normal faulting mechanisms. However, the strikes of the nodal planes are different. This was also the case with the main event of the Rampart sequence. This discrepancy was discussed by Chung and Kanamori (1978). Their argument was outlined earlier in this paper and will not be discussed here. The final mechanism is shown in Figure 23.

The earthquake occurred in the north-central Kigluaik Mountains of Seward Peninsula, an east-west trending arch of Precambrian gneiss. The area is heavily faulted. Nakamura et al. (1980) discusses the Bendelben and Kigluaik faults in the southern portion of the peninsula (see Figure 3). They define a normal fault system 175 km long which shows large amounts of Cenozoic dip-slip displacement (Nakamura et al., 1980). The Seward Peninsula event occurred on the Kigluaik fault. The mechanism determined in this study agrees well with the observed normal faulting in the area.

Event 8

One of the more thoroughly studied earthquakes in central Alaska is

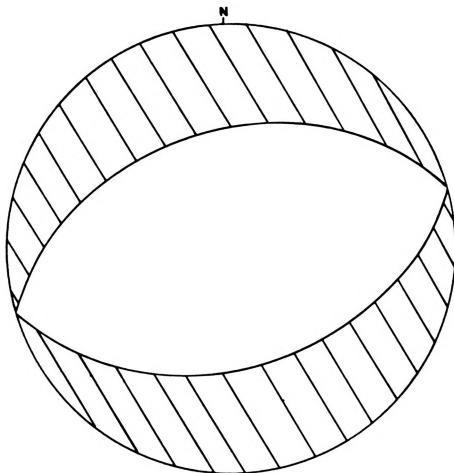


FIGURE 23
FINAL MECHANISM SOLUTION FOR EVENT 7

a magnitude 5.8 event with epicentral coordinates of 64.7N, 160.2W. Sykes and Sbar (1974) used first motion data and S-wave polarization angles for their study. They concluded the earthquake had a normal faulting mechanism with the B-axis trending N55W and lying nearly horizontal. Their data are shown in Figure 24A. Liu and Kanamori (1980) arrived at the same solution after calculating synthetic seismograms for 20 different stations. Their solution is shown in Figure 24B. Two similarities exist between this event and the Seward Peninsula earthquake. First, the B-axis in both events is nearly horizontal. Secondly, neither event has an aftershock sequence, which is contrary to what many of the other larger intraplate earthquakes in Alaska exhibit.

Events 9 and 10

Events 9 and 10 occurred to the north of the Seward Peninsula, one near the tip of Baldwin Peninsula in Kotzebue Sound and the other in the western Brooks Range. Both have nearly identical focal mechanisms. Event 9 was a magnitude 5.2 event which occurred on 81-7-12. It was recorded at 161 seismic stations and has an epicentral location of 67.71N, 161.20W. A small foreshock and aftershock sequence consisting of 16 events is associated with the main shock. First motion data from the ISC Bulletin for the main event are plotted in Figure 25. A strike-slip mechanism with nearly vertical focal planes fits the data well.

The foreshock and aftershock sequences were relocated using the master event technique. Figure 26A and B show epicentral locations before and after relocation, respectively. The trend of epicenters after relocation is N70W which suggests that the N74W striking nodal plane is

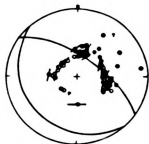


FIGURE 24A

FOCAL MECHANISM SOLUTION FOR EVENT 8: AFTER SYKES AND SBAR (1974)

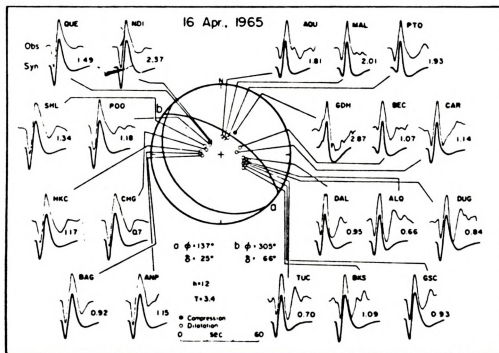


FIGURE 24B

FOCAL MECHANISM SOLUTION FOR EVENT 8: AFTER LIU AND KANAMORI (1980)

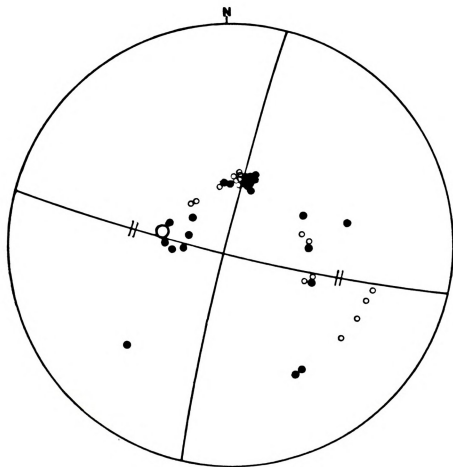


FIGURE 25

FIRST MOTION DATA OF EVENT 9

The dilatation at 285° azimuth is a short and long period dilatation reported in the ISC Bulletin.

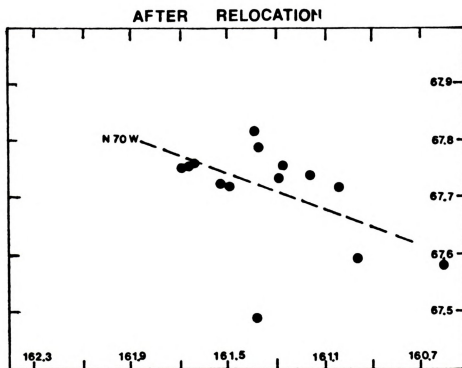
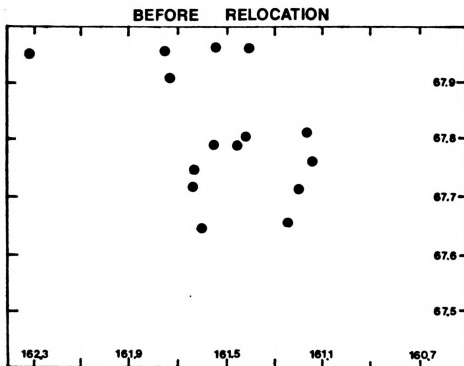


FIGURE 26

AFTERSHOCK RELOCATION OF EVENT 9

has exhibited signs of activity in recent geologic time (Brogan et al., 1975) and which has about the same N74W strike as the fault plane.

Event 10 occurred on 66-8-26 and was a moderate magnitude 5.0 event. It occurred at 66.71N, 162.7W and was recorded by 82 seismic stations. First motion data read from WWSSN records, the Canadian Seismograph Network and reported in the ISC Bulletin are plotted in Figure 27. The nodal planes are fairly well constrained and show a strike-slip mechanism nearly identical to the previously described event. No data is available which would definitely determine the fault plane. However, the geologic structures in southwest Hope Basin have east-west orientations (Grantz et al., 1975). There are also two east-west seismicity trends within Kotzebue Sound (Biswas et al., 1980). This evidence, along with the focal mechanism similarity with event 8, suggests that the east-west plane is the fault plane.

Events 11 and 12

Focal mechanisms were determined for two sequences on the west end of Seward Peninsula. Mechanism 11 is a composite mechanism of four events which occurred near the northern coastline (see Table 1). Two of the four events occur at the same location (65.9N, 167.0W) while the other's are located 50 km to the north and 50 km to the south. Even though the latter two events occur a considerable distance from the first two, they are included in the composite for two reasons. First, each of the distant events occur in conjunction with one of the central events. Secondly, the first motion data reported in the ISS from all of the events are consistent and result in the focal mechanism shown in Figure 28.

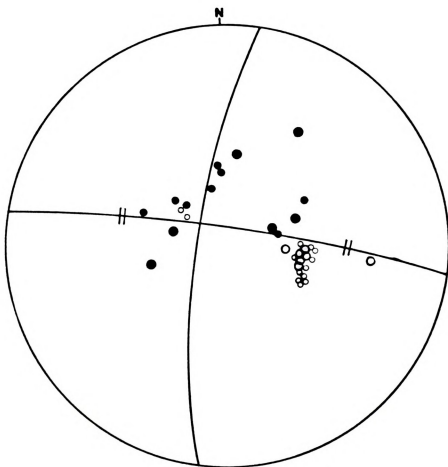


FIGURE 27
FIRST MOTION DATA OF EVENT 10

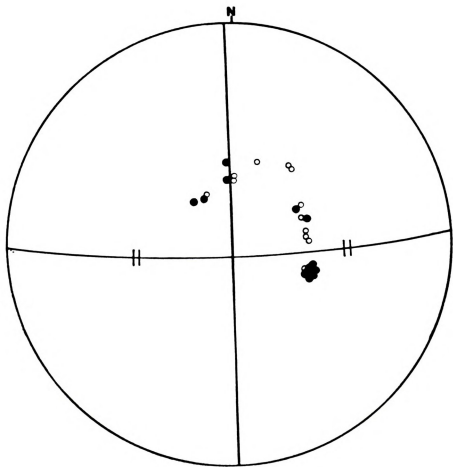


FIGURE 28
COMPOSITE FIRST MOTION DATA FOR EVENTS 11

Event 12 occurred on 64-6-11 and had a magnitude of 5.0. It's epicenter was on the most western point of Seward Peninsula at 65.35N, 168.3W and was recorded by 61 seismic stations. First motion data reported in the ISC Bulletin are used for the focal mechanism shown in Figure 29. This gives a mechanism similar to that of event 11 discussed in the previous paragraph. Biswas et al. (1980) note that east-west fault trends and seismicity trends have been mapped in the area which lends support to the proposal that the east-west striking nodal plane is the fault plane. If the fault plane is assumed to be correct, then the proposed north-south nodal plane is reasonably well constrained by the given data.

Huslia Series (Events 13 and 14) and Event 15

The earthquake which occurred on 58-4-7 at 15.30.40 (event 13, Table 1) was the largest event (magnitude=7.3) of a series of earthquakes which are hereafter referred to as the Huslia series. An aftershock sequence of greater than 50 events followed the main shock (Davis, 1960). Two of the aftershocks, one of which was event 14 (58-4-13 at 9.7.24) were reported in the ISS and were of magnitude 6.5. First motion data from the ISS for events 13 and 14 were used in an attempt to constrain the focal mechanisms. A focal mechanism constraint for the third large magnitude event of the series was not possible due to the lack and inconsistency of the first motion data reported in the ISS. The data for event 14 allows for two possible solutions, a normal fault and a reverse fault. Both are shown in Figure 30. First motion data for event 13, the main event of the series, are shown in Figure 31. The data are too inconsistent to allow any constraints to be placed upon a focal mechanism.

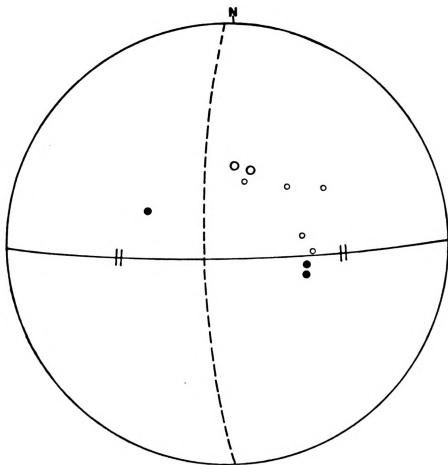


FIGURE 29
FIRST MOTION DATA OF EVENT 12

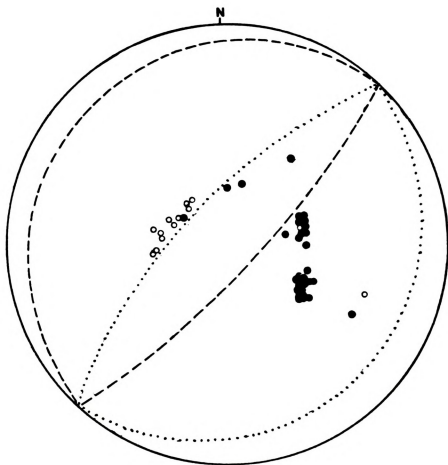


FIGURE 30
FIRST MOTION DATA OF EVENT 14 FROM THE ISS

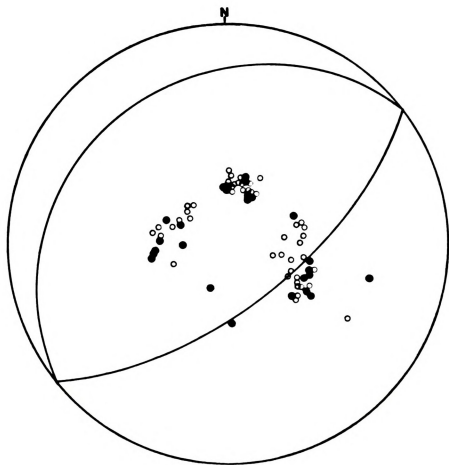


FIGURE 31
FIRST MOTION DATA OF EVENT 13 FROM THE ISS

Four mechanisms have been proposed by other authors for event 13. Three of the mechanisms (Schaffner, 1961; Balakina, 1962; and Stevens, 1964) are shown in Figure 32 and are predominantly strike-slip. The mechanism proposed by Ritsema (1962) is for a normal fault and is shown in Figure 33. Ritsema used first motion data read from seismic records as well as S-wave polarization angles. The southeasterly dipping plane is well constrained by the first motion data. The S-wave polarization data fit a plane trending N46E and dipping 36 degrees to the northwest. This focal mechanism is very similar to the normal mechanism proposed for event 14. It is preferred to the solutions of Schaffner (1961), Balakina (1962) and Stevens (1964) since the nodal planes are well constrained by Ritsema's (1962) data. In addition, the agreement with the proposed normal faulting mechanism for event 14 and with field data gathered by Davis (1960), which will be discussed momentarily, suggest it is the preferred mechanism.

It should be noted that the orientation of the northwest dipping plane determined in this study is different from that which Ritsema (1962) proposed. The plane used in the Ritsema study is consistent with the first motion data but not the S-wave polarization angles. However, Ritsema was trying to prove a single couple mechanism for the event and did not attempt to fit nodal planes with differing orientations to the data. Ritsema (1962) used the polarization angles as an argument against a possible northwest dipping nodal plane. The northwest dipping nodal plane suggested in this study is in good agreement with the Ritsema (1962) data.

In a field report for the Huslia series (Davis, 1960), Davis took measurements of the vertical displacement on 35 fissures parallel to the

FIGURE 32

PROPOSED MECHANISMS FOR EVENT 13

Schaffner (1961); solid lines with hachures
Balakina (1962); dot-dashed lines with hachures
Stevens (1964); dotted lines

The hachures marks on the mechanisms of Schaffner and Balakina point into the compressional quadrants.

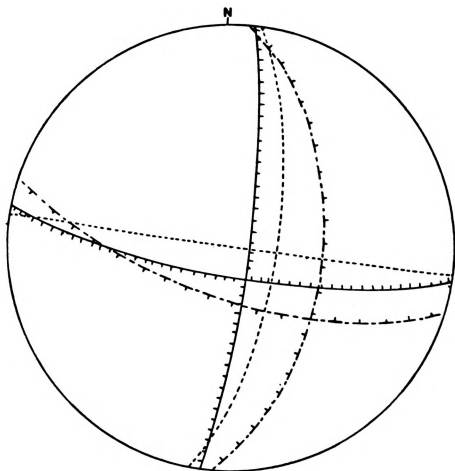


FIGURE 32

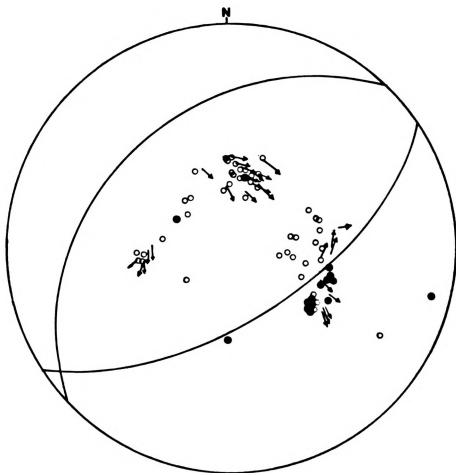


FIGURE 33
FIRST MOTION AND S-WAVE POLARIZATION ANGLE DATA OF EVENT 13

epicentral zone and found a net downward movement on the northwest side of the faults relative to the southeast side. This is in agreement with the proposed normal focal mechanism and would require the northwest dipping nodal plane to be the fault plane. However, two other pieces of data suggest the southeast dipping nodal plane to be the fault plane. The fissures on which the displacement measurements were taken had trends averaging N56E, which is close to the N58E strike of the southeast dipping nodal plane. In addition, Brogan et al. (1975) note that the Huslia fault is observed near the epicentral zone of the Huslia series. The N70E trend of the fault is closer to the N58E strike of the southeast dipping plane than the N46E strike of the northwest dipping plane. Determination of the fault plane is not attempted due to the contradictory evidence available.

On 58-5-10 and on 58-5-11, about one month after the Huslia series, two magnitude 6.3 earthquakes occurred with epicentral coordinates of 65.23N, 152.01W, and 65.1N, 151.9W respectively. The location is approximately 260 km to the southeast of the Huslia series. The first motion data for event 15 (the 58-5-10 event) were obtained from the ISS and are shown in Figure 34. The earthquake epicenter is located on the Kaltag fault, a 440 km long strike-slip fault in west central Alaska. The Kaltag fault has a N80E strike at the epicenter, which is close to the N75E nodal plane. Thus, it is probable that the Kaltag fault is the fault plane. The second nodal plane cannot be constrained with any degree of accuracy. Regardless of its orientation, the first motion data will not allow a pure strike-slip focal mechanism solution. A large component must be either thrust or normal faulting.

It is curious that two large series of earthquakes separated by 250

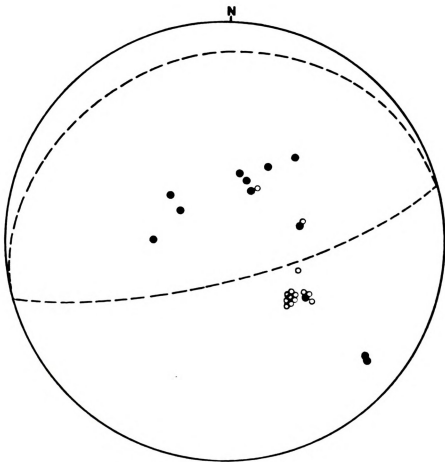
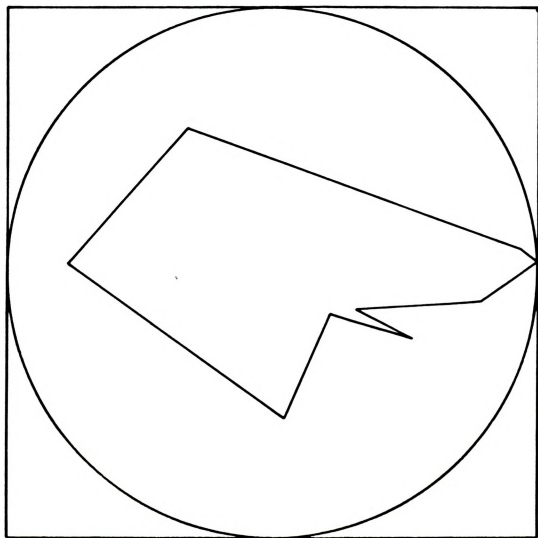


FIGURE 34
FIRST MOTION DATA OF EVENT 15

km should occur within a month of each other. It may be due to a large scale reorientation of the stress field within Alaska. In 1957 an extremely powerful earthquake (magnitude=8.0) occurred in the Aleutian arc on 57-3-9. It was strong enough to be recorded at 365 stations. An aftershock sequence of 135 earthquakes over the following week occurred along a 1000 km section of the Aleutian Arc (Rothe, 1969). Such a large magnitude main event and the extremely widespread aftershock sequence would have some impact on the regional stress field. The 1958 events in central Alaska may have been one outcome of this.

Caro (Event 16)

The Caro series consisted of two earthquakes which occurred on 66-12-20 at 00.26.28 and at 00.57.53. The epicenters were located at 66.82N, 148.1W and 66.79N, 148.4W and were of magnitudes 4.8 and 4.9 respectively. No aftershocks were reported. An attempt to calculate the Rayleigh wave radiation pattern was made. However, the magnitude of the events were not large enough to enable the recording of good long period records at more than 9 stations. The Rayleigh wave data from 9 stations for the first event of the pair are plotted in Figure 35. The pattern does not offer any constraints on the nodal planes. First motions from the ISC Bulletin and read from WWSSN and Canadian Network seismic records enable a focal mechanism to be determined for the event at 00.57.53. It is shown in Figure 36. The mechanism for the other event is assumed to be the same due to the striking similarities of their long period seismic wave forms. Figure 37 shows the record of both events recorded at College, Alaska. The first 60 seconds of each signal are nearly identical. The geologic map of Alaska (Beikman, 1980) shows the general fault pattern of



PERIOD=30 SEC.

FIGURE 35
RAYLEIGH WAVE RADIATION PATTERN FOR EVENT 16

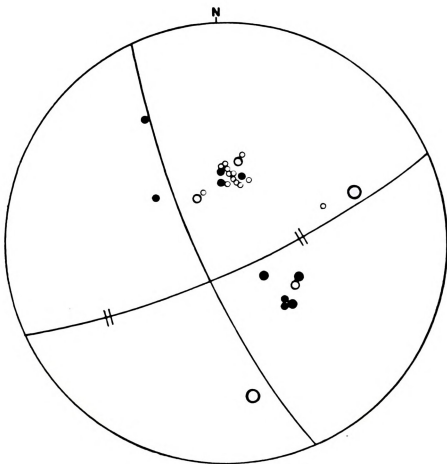


FIGURE 36

FIRST MOTION DATA OF EVENT 16

FIGURE 37

SEISMIC RECORD AT STATION "COL" FOR EVENT 16

The left record is from the event 66-12-20 at 00.26.28; the right record is from the event of 66-12-20 at 00.57.54.

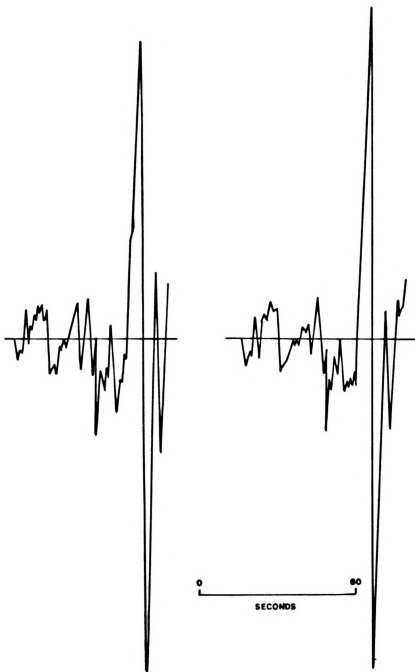


FIGURE 37

the area to trend N55E which is close to the N60E trending nodal plane.
As a best approximation then, the N60E plane is picked as the fault plane.

DISCUSSION

The focal mechanisms from this study are shown in Figure 38 and are summarized in Table 2. It was found that the majority of Alaskan and Chukotka intraplate seismicity is associated with pre-existing faults. The Rampart series (events 1 and 2) and the event on Seward Peninsula are two examples of this. McKenzie (1969) suggested that shallow earthquakes will occur along planes of weakness in the crust. The McKenzie study found that the P-axis orientation determined by a focal mechanism is only weakly controlled by the greatest principle stress direction (S_2). The S_1 direction need only lie in the same quadrant as the P-axis and may be nearly perpendicular to it (McKenzie, 1969). This suggests that pre-existing faults will be the overriding factor in determining the location of shallow earthquakes. It has also been shown that shear stresses involved in shallow earthquakes are too small to produce new fractures (Chinnery, 1964; Brune and Allen, 1967). Thus, the stresses that build up in the shallow crust will be released on pre-existing faults.

Sykes (1978) found that many intraplate regions which exhibit seismic activity such as Britain and the Appalachians occur in areas of pre-existing faults or fold belts which parallel the continental margins. The geologic map of Alaska (Beikman, 1980) shows that Alaska exhibits this same structural style. The model that Sykes (1978) proposes which best explains the intraplate seismicity of Alaska is one in which a relatively weak area, in this case central Alaska, is compressed between

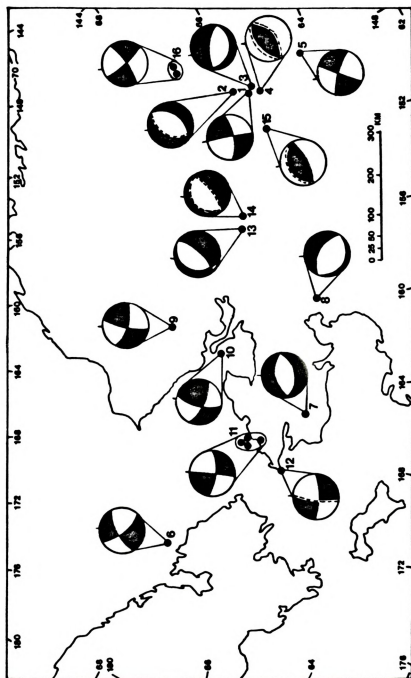


FIGURE 38
FOCAL MECHANISM DISTRIBUTION

TABLE 2

LIST OF FOCAL MECHANISMS

Event Number	Focal Mechanism Plane 1 (str/Dip)	Plane 2 (str/Dip)	Constraint	Type of Mechanism	MHS Orientation (Az)	MHS Axis	Aftershock Sequence
1	N8E/90*	N82W/80S	G	S-S	334	S1	Yes
2	N45E/45NW	N45E/45SE	P	N	319	S2	---
3	N82W/60N	N68W/22S	G	N	360	S2	No
4	N45E/45NW	N45E/45SE	P	R	335	S1	No
5	N33E/90*	N56W/80NE	F	S-S	8	S1	No
6	N48W/85SW*	N44E/74NW	P	S-S or N	282	S1	No
7	N76E/45NW	N76E/45SE	G	N	333	S2	No
8	N40W/30SW	N56W/62NE	G	N	28	S2	No
9	N74W/85S*	N16E/87NW	G	S-S	309	S1	Yes
10	N80W/84N*	N10E/80W	G	S-S	331	S1	No
11	N88E/83S*	N2W/90	F	S-S	65	S1	No
12	N88E/84S*	N2W/80W	P	S-S	52	S1	No
13	N46E/36NW	N58E/63SE	G	N	327	S2	Yes
14	Not Constrained			N or R	328	S2	---

TABLE 2
(continued)
LIST OF FOCAL MECHANISMS

Event Number	Focal Mechanism		Constraint	Type of Mechanism	MHS Orientation (Az)	MHS Axis	Aftershock Sequence
	Plane 1 (str/Dip)	Plane 2 (str/Dip)					
15	N75E/15N	N75E/75S	P	R	337	S ₁	No
16	N60E/80SE*	N32E/80SW	F	S-S	360	S ₁	No

* signifies the fault plane

Constraint: G-good F-fair P-poor

Type: S-S-strike slip N-normal R-reverse

two stronger blocks, the stronger blocks being the area north of the Brooks Range (the North Slope) and the oceanic lithosphere south of the Aleutian trench. Sykes (1978) points out that while oceanic lithosphere is thinner and therefore considered weaker than continental crust, the strength of the continental crust may be greatly reduced if it is highly faulted. Many regions of Alaska, particularly the area surrounding the Rampart series, exhibit this characteristic.

The above model accounts for intraplate seismicity which occurs in heavily faulted areas such as central Alaska and Seward Peninsula. However, other areas in central Alaska which are seismically active do not have such a heavily faulted character. An example of this is the high level of seismicity observed in the central and southern Yukon-Koyukuk province. Only a few minor faults are shown on the geologic map of Alaska for this region and topographic maps show no linear features typical of a fault's surface expression.

A possible explanation can be drawn from work done by Nakamura and Uyeda (1980) and Nakamura et al. (1977, 1980). Nakamura mapped the orientation of the maximum horizontal compression (MHC), and whether it was S_1 (axis of greatest stress) or S_2 (axis of intermediate stress) in southern Alaska and the eastern Bering Sea. The directions were determined by measuring dike swarm trends associated with volcanoes and stress orientations needed to produce the observed movement on recently active faults. The MHC orientations from Nakamura et al. (1980) are shown in Figure 39. Along the Aleutian arc the MHC direction is parallel to the direction of plate motion. In central Alaska this orientation begins to vary and tends to form a fan shaped pattern with the line of symmetry trending approximately N25-30W from the eastern end of the Aleutian trend.

FIGURE 39

MAXIMUM HORIZONTAL COMPRESSION (MHC) FROM NAKAMURA AND UYEDA (1980)

The wide spaced double line separates the primarily compressional area in central Alaska from the primarily extensional area in western Alaska and the Bering Sea. The thin double line with the hachures map the MHC orientations. The large arrows are in the direction of motion of the oceanic lithosphere subducting in the Aleutian trench.

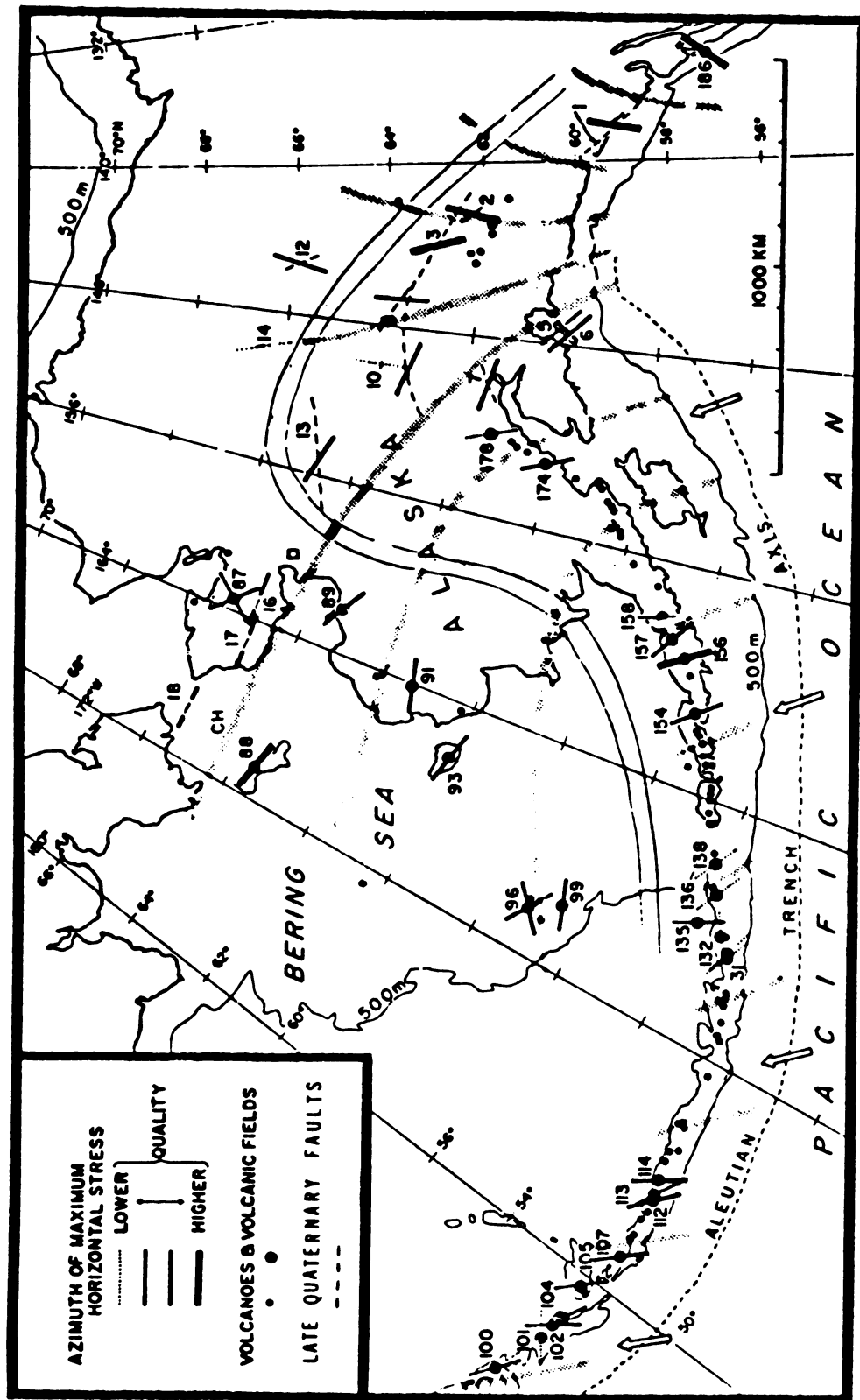


FIGURE 39

Stress orientations can also be estimated from focal mechanisms. This is done by using the P and T axis to determine the S_1 and S_3 (axis of minimum stress) directions respectively. As previously mentioned (McKenzie, 1969), this assumption is not necessarily valid. However, Rayleigh et al. (1972) have shown that new faults will be created in areas where existing faults are in unfavorable orientations. Their experiments showed that only pre-existing planes of weakness lying between approximately 10 and 50 degrees of S_1 would slip. Thus if the P-axis is assumed to lie at 45 degrees to the fault plane, the error in using the P-axis as an estimation of the S_1 direction is a maximum of 35 to 40 degrees. If the fault plane can be determined, the error can be reduced to 20 degrees. The MHC orientations determined from this study are plotted in Figure 40. They generally show good agreement with Nakamura's data.

Another conclusion that Nakamura reached is that the MHC axis tends to change from S_1 in central and southern Alaska to S_2 in western Alaska and the Bering Sea. The two regions are separated by the double line in Figure 39. Nakamura equates this as being a change from a predominantly compressional environment in southern and central Alaska to an extensional one in western Alaska and the eastern Bering Sea. The compressional forces are probably caused by compression along the Aleutian arc and the transmittance of these forces to the interior of Alaska. The extensional forces may be caused by an upward movement of asthenospheric material, the same mechanism postulated for back-arc spreading (Nakamura et al., 1980). It is also noted that the boundary between the differing stress regimes corresponds to the boundary separating two different types of volcanism. Polygenetic calc-alkaline volcanics are dominant in the

FIGURE 40

MHC ORIENTATIONS FROM FOCAL MECHANISMS

The wide spaced double line and thin, hachured double lines are from Nakamura et al. (1980). The solid lines are MHC orientations where S_1 is the MHC. The dashed lines are MHC orientations where S_3 is the MHC.

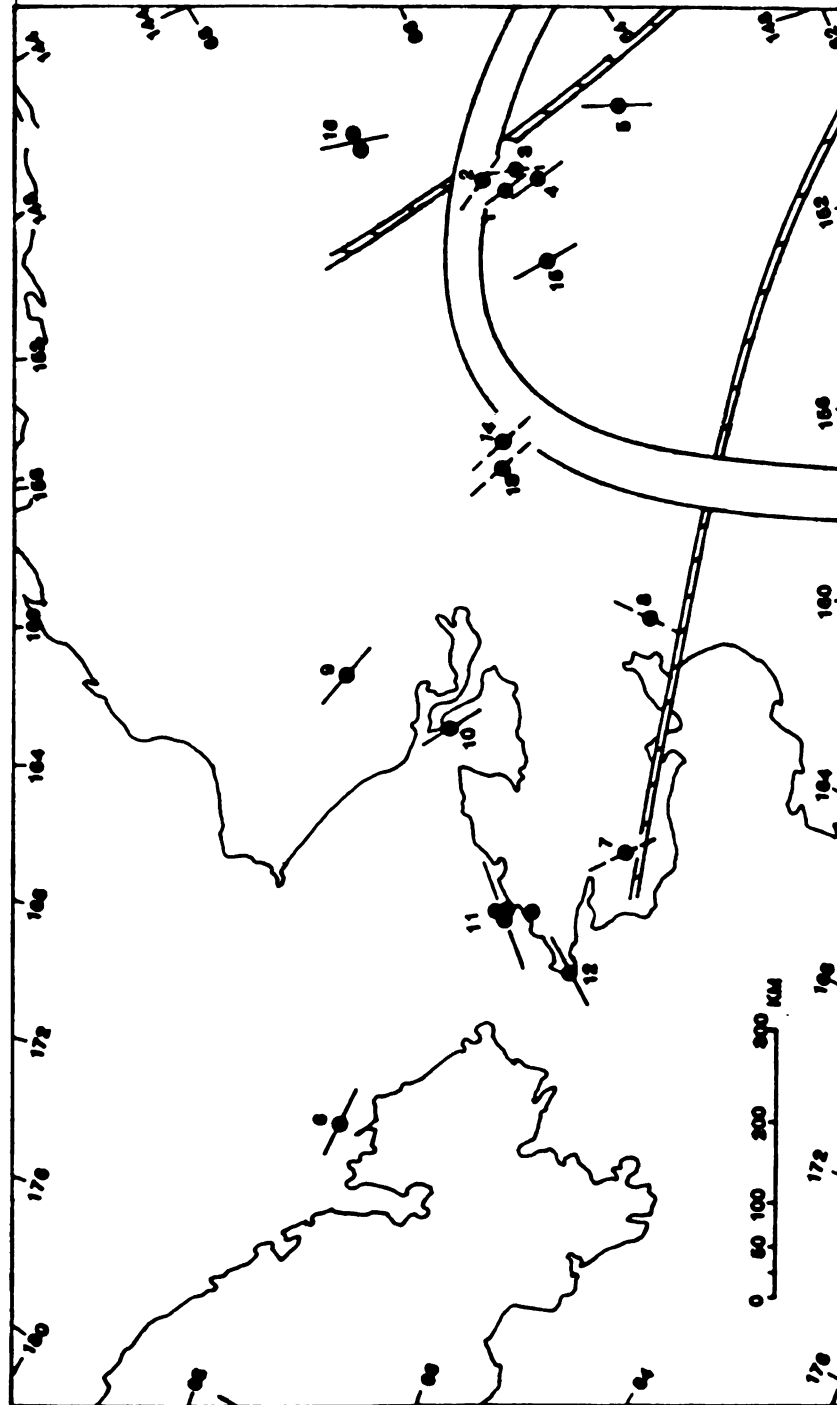


FIGURE 40

southern, compressive zone whereas monogenitic alkali-basaltic volcanics are more predominant in the northern, extensional region (Nakamura et al., 1980). Even though extensional forces are predominant in the northern zone, active spreading in the back-arc area is not observed. It is possible that spreading will not occur unless there is a lessening of compressional stresses at the arc or trench (Nakamura et al., 1980). Regardless of the mechanism, the observed extensional forces are the probable causes of the large magnitude normal mechanism earthquakes which occur in the Yukon-Koyukuk (events 8 and 13) and on Seward Peninsula (event 7). Recent work by Fujita et al. (1983) has shown that the focal mechanism for the Chukotka earthquake (event 6) may also be a normal fault with east-west striking nodal planes.

Figure 40 is plotted slightly different than the Nakamura data (Figure 39). For the normal fault mechanisms in which the S_2 axis is the MHC, the S_3 axis is plotted. The S_3 axis should be a better indicator of an extensional stress regime than the S_2 axis, which is what Nakamura et al. (1980) mapped. The S_1 and S_3 axis determined from this study show good agreement with the Nakamura et al. (1980) data near the boundary between the compressional and extensional regimes. To the west of this boundary the data is in poor agreement with Nakamura's model. Even if the S_2 axis for the normal mechanism events are plotted, the axis orientations still do not agree with the Nakamura data. However, all of the mechanisms in the area are either strike-slip or normal fault mechanisms which agree with the general conclusion that the stress regime in Alaska and the Bering Sea is typified by extensional forces.

An observation should be noted. The larger earthquakes which occurred in central Alaska, such as the Rampart series and the Huslia series,

each had large aftershocks sequences associated with them. The large magnitude events in other areas occurred either as earthquake pairs (the Caro and Seward Peninsula events) or as single isolated events (event 8 and the Chukchi earthquake).

The two types of events have a distribution which roughly corresponds to the compressional and extensional zones described by Nakamura et al. (1980). The events with aftershock sequences fall within or near to the compressional zone while the events with no aftershocks fall within the extensional zone. The two events in the Huslia series occurred on the border between the two zones and exhibit characteristics of both; the normal fault mechanism corresponds to the northern extensional zone and it has the aftershock sequence typical of southern zone earthquakes.

It should also be noted that event 9 does not fit this pattern. It is a large event of magnitude 5.2 which occurred in the northern zone. However, it is associated with a foreshock and aftershock sequence consisting of 16 events. Event 6 had an aftershock series of 50 events (Lazareva, 1970) and also occurred in the northern zone. However, all were of very low magnitude and were recorded by a local station in northeast Siberia while the aftershock series of the Alaskan events were of great enough magnitude to be reported in the ISC Bulletin.

CONCLUSIONS

Central Alaska and Chukotka has been shown to be a very seismically active intraplate region. This study placed constraints upon the focal mechanisms of 12 of the area's earthquakes. An additional four mechanisms from other authors supplemented this data set. The majority of the earthquakes studied are associated with pre-existing faults. However, some of the events occurred in areas where faulting is not known to exist. A possible explanation for this lies in work done by Nakamura et al., (1977, 1980). Nakamura found that the maximum horizontal compression (MHC) direction determined from dike swarm orientations and recent fault movement form a fan shaped pattern across central Alaska. The occurrences of earthquakes in the unfaulted areas of Alaska are generally related to the two stress regimes of Nakamura et al., (1977, 1980).

BIBLIOGRAPHY

BIBLIOGRAPHY

Balakina, L.M., 1962: General regularities in the direction of the principal stresses effective in the earthquake foci of the seismic belt of the Pacific Ocean, Izu. AN SSSR Ser. Geof., p. 1471-1483 (English Transl. by Amer. Geophys. Union).

Beikman, H.M., 1980: Geologic Map of Alaska, U.S. Geol. Sur., 1:2,500,000, 2 sheets.

Berg, H.C., D.L. Jones and P.J. Coney, 1978: Map showing pre-Cenozoic Tectonostratigraphic terrains of southeastern Alaska and adjacent areas, U.S. Geol. Sur. Open File Report 78-1085.

Bhattacharya, B. and N.N. Biswas, 1979: Implications of N. Pacific plate tectonics in Central Alaska: Focal mechanisms of earthquakes, Tectonophysics, v. 53, p. 99-130.

Biswas, N.N., L. Gedney and J. Agnew, 1980: Seismicity of Western Alaska, Bull. Seismol. Soc. Amer., v. 70, p. 873-884.

Bramhall, E.H., 1938: The central Alaska earthquake of July 22, 1937, Bull. Seismol. Soc. Amer., v. 28, p. 71-75.

Brogan, G.E., L.S. Cluff, M.K. Korringa, and D.B. Slemmons, 1975: Active faults of Alaska, Tectonophysics, v. 29, p. 73-85.

Brune, J.N. and C.R. Allen, 1967: A low-stress-drop low magnitude earthquake with surface faulting: the Imperial, California earthquake of March 4, 1966, Bull. Seis. Soc. Amer., v. 57, p. 501-514.

Chinnery, M.A., 1964: The strength of the earth's crust under horizontal shear stress, J. Geophys. Res., v. 65, p. 675-693.

Chung, W.Y. and H. Kanamori, 1978: Subduction processes of a fracture zone and aseismic ridges - The focal mechanism and source characteristics of the New Hebrides earthquakes of January 19, 1969 and some related events, Geophys. J. Royal Ast. Soc., v. 54, p. 221-240.

Churkin, M., W.J. Nokleberg and C. Huie, 1979: Collision-deformed Paleozoic continental margin, Western Brooks Range, Alaska, Geology, v. 7, p. 379-383.

Churkin, M., C. Carter, and J.H. Trexler, 1980: Collision deformed Paleozoic continental margin-foundation for microplate accretion, Geol. Soc. Amer. Bull., v. 91, p. 648-654.

- Collier, A.J., 1902: A reconnaissance of the northwestern portion of Seward Peninsula, Alaska, U.S. Geol. Sur. Prof. Paper #2, 70p.
- Davis, T.N., 1960: A field report on the Alaska earthquakes of April 7, 1958, Bull. Seismol. Soc. Amer., v. 50, p. 489-510.
- Everenden, J.F., 1969: Identification of earthquakes and explosions by use of teleseismic data, J. Geophys. Res., v. 74, p. 3828-3856.
- Freeland, G.L. and R.S. Dietz, 1973: Rotation history of Alaskan tectonic blocks, Tectonophysics, v. 18, p. 379-389.
- Fujita, K. and J.T. Newberry, 1982: Tectonic evolution of northeast Siberia and adjacent regions, Tectonophysics, v. 89, p. 337-357.
- Fujita, K., D.B. Cook and M.J. Coley, 1983: Tectonics of the western Beaufort and Chukchi seas, EOS, v. 64, p. 163.
- Fujita, K. and J.T. Newberry, 1983: Accretionary terrains and tectonic evolution of northeast Siberia, Hashimoto, M. and Uyeda, S. editors, Accretion Tectonics in Circum Pacific Regions, Terra Scientific Pub. Co., Tokyo, p. 39-53.
- Gedney, L. and E. Berg, 1969a: Some characteristics of the tectonic stress pattern in Alaska, Geophys. J. Royal. Ast. Soc., v. 17, p. 293-304.
- Gedney, L. and E. Berg, 1969b: The Fairbanks earthquakes of June 21, 1967: Aftershock distribution, focal mechanisms, and crustal parameters, Bull. Seismol. Soc. Amer., v. 59, p. 73-100.
- Gedney, L., 1970: Tectonic stresses in S. Alaska in relationship to regional seismicity and the new global tectonics, Bull. Seis. Soc. Amer., v. 60, p. 1789-1802.
- Gedney, L., S. Estes, and N. Biswas, 1980: Earthquake migration in the Fairbanks, Alaska seismic zone, Bull. Seis. Soc. Amer., v. 70, p. 223-241.
- Goryachev, A.V., N.V. Kondorskaya and N.S. Landyreva, 1968: The Chukchi Peninsula and the Koryak Range, from Seismic Zoning of the USSR, ed. S.V. Medvedev, Moscow, p. 498-501.
- Grantz, A., 1966: Strike slip faults in Alaska, U.S. Geol. Sur. Open File Report 66-267.
- Grantz, A., M.L. Holms and B.A. Kososki, 1975: Geologic framework of the Alaskan Continental terrace in the Chukchi and Beaufort Seas, U.S. Geol. Sur. Open File Report #75, 124p.
- Herrmann, R.B., 1975: A students guide to the use of P and S wave data for focal mechanism determination, Earthquake Notes E. Sec. Seis. Soc. Amer., v. 46, p. 29-39.

Hudson, T., 1977: Geologic map of Seward Penn., Alaska, U.S. Geol. Sur. Map 77-796A.

Jones, D.L., N.J. Silberling, and J. Hillhouse, 1977: Wrangellia-a displaced terrain in northwestern North America, Can. J. of Earth Sci., v. 11, p. 2565-2577.

Jones, D.L. and N.J. Silberling, 1979: Mesozoic stratigraphy-the key to tectonic analysis of S. and central Alaska, U.S. Geol. Sur. Open File Report 79-1200.

Jones, D.L., N.J. Silberling, H.C. Berg, and G. Plafker, 1981: Map showing tectonostratigraphic terrains of Alaska, columnar sections, and summary description of terrains, U.S. Geol. Sur. Open File Report 81-792, 20p. with maps.

Kanamori, H., 1970: The Alaska earthquake of 1964: radiation of long-period surface waves and source mechanism, J. Geophys. Res., v. 75, p. 5029-5040.

Kanamori, H. and G.S. Stewart, 1976: Mode of strain release along the Gibbs fracture zone, Mid-Atlantic ridge, Phys. Earth Planet Interiors, v. 11, p. 312-332.

Kondorskaya, N.V. and Shebalin, 1977: Novii Katalog Sil'nikh Zemletryasenii na Territorii SSSR, Akademiya Nauk SSSR, Moskva, 536p.

Lazareva, A.P., 1970: Zemletryaseniya Arktiki v 1970; 1971gg (Arctic Earthquakes of 1970 and 1971), Zemletryaseniya v SSSR v 1971, Godu p. 145-149 (in Russian).

Liu, H.L. and H. Kanamori, 1980: Determination of source parameters of mid-plate earthquakes from waveforms of body waves, Bull. Seis. Soc. Amer., v. 70, p. 1989-2004.

Martin, A.J., 1970: Structure and tectonic history of the Western Brooks Range, DeLong Mts., and Lisburne Hills, northern Alaska, Geol. Soc. Amer. Bull., v. 81, p. 3605-3622.

McKenzie, D.P., 1969: The relation between fault plane solutions for earthquakes and the directions of the principal stress, Bull. Seis. Soc. Amer., v. 59, p. 591-601.

Nakamura, K., K.H. Jacob and J.N. Davies, 1977: Volcanoes as possible indicators of tectonic stress orientation-Aleutians and Alaska, Pure Applied Geophys., v. 115, p. 87-112.

Nakamura, K. and Uyeda, 1980: Stress gradient in arc back-arc regions and plate subduction, J. Geophys. Res., v. 85, p. 6419-6428.

Nakamura, K., G. Plafker, K.H. Jacob and J.N. Davies, 1980: A tectonic stress trajectory map of Alaska using information from volcanoes and faults, Bull. Earthquake Res. Inst., v. 55, p. 89-100.

Patton, W.M. and J.M. Hoare, 1968: The Kaltag fault, West Central Alaska, U.S. Geol. Sur. Prof. Paper #600D, p. D147-D153.

Patton, W.W., 1973: Reconnaissance geology of the Northern Yukon-Koyukuk Province, Alaska, U.S. Geol. Sur. Prof. Paper 774-A, 17p.

Patton, W.A., I.L. Tailleir, W.P. Brosge and M.A. Lamphere, 1977: Preliminary report on the ophiolites of Northern and Western Alaska, North American Ophiolites, State of Oregon Dept. of Geology and Mineral Industries, edited by R.G. Coleman and W.P. Irwin, p. 51-57.

Pho, H. and L. Behe, 1972: Extended distances and angles of incidence of P-waves, Bull. Seis. Soc. Amer., v. 62, p. 885-902.

Rayleigh et al., 1972: in Flow and Fracture of Rocks, Amer. Geophys. Union Geophys. Res., Mon. Series, ed. Heard, v. 16, p. 275-284.

Richardson, R.M., S.C. Solomon, and N.H. Sleep, 1976: Intraplate stresses as an indicator of plate tectonics driving forces, J. Geophys. Res., v. 81, p. 1847-1856.

Ritsema, A.R., 1962: P and S amplitudes of two earthquakes of the single couple type, Bull. Seis. Soc. Amer., v. 52, p. 723-746.

Rothe, J.P., 1969: Seismicity of the Earth: 1953-1965, United Nations Educational, Scientific, and Cultural Organization, Paris, 336p.

Sainsbury, G.L., 1969: Geology and ore deposits of the central York Mountains, Seward Peninsula, Alaska, U.S. Geol. Sur. Bull., v. 12, p. 1287.

Sainsbury, G.L., R.G. Coleman and R. Kachadoorian, 1970: Blueschist and related greenschist facies rocks of the Seward Penn., Alaska, U.S. Geol. Sur. Prof. Paper 700-B, p. B33-B42.

Schaffner, H.J., 1961: Tabillen Kinematischen Erdhebenherdparameters, Pub. Inst. Agnew, Geophysik, Freiberg.

Snelson, S. and I.L. Tailleir, 1968: Large-scale thrusting and migrating Cretaceous fore-deep in the Western Brooks Range and adjacent areas of northwestern Alaska (abs.) Pacific Sec. Amer. Assoc. Pet. Geol. 43rd Ann. Meet., p. 12.

St. Amand, P., 1948: The central Alaska earthquake swarm of October 1947, Trans. Amer. Geophys. Union, v. 29, p. 613-623.

Stein, S., and E.A. Okal, 1978: Seismicity and tectonics of the Ninetyeast Ridge: evidence for internal deformation of the Indian plate, J. Geophys. Res., v. 83, p. 2233-2246.

Stevens, A.E., 1964: Earthquake mechanism determination by S-wave data, Bull. Seis. Soc. Amer., v. 54, p. 457-474.

Sykes, L.R., and M.L. Sbar, 1974: Focal mechanism solutions of intraplate earthquakes and stresses in the lithosphere, Geodynamics of Iceland and the North Atlantic Area, D. Reidel Publishing, Holland, 323p.

Sykes, L.R., 1978: Intraplate seismicity, reactivation of pre-existing zones of weakness, alkaline magmatism, and other tectonism postdating continental fragmentation, Rev. Geophys. Space Phys., v. 16, p. 621-688.

VanWormer, J.D., J. Davies, and L. Gedney, 1974: Seismicity and plate tectonics in south central Alaska, Bull. Seismol. Soc. Amer., v. 64, p. 1467-1475.

Voyevodin, V.N. and K.S. Sukhov, 1977: Tectonics, Magmatism and Metallogeny of the Mesozides of Eastern Chukotka: Int. Geol. Rev., v. 19, p. 728-736.

Wang, S., R.J. Geller, and S. Stein, 1979: An intraplate thrust earthquake in the South China Sea, J. Geophys. Res., v. 84, p. 5627-5631.

Weaver, C. and D. Hill, 1978/79: Earthquake swarms and local crustal spreading along major strike-slip faults in California, Pure Applied Geophys., v. 117, p. 51-64.

Zoback, M.L., and M. Zoback, 1980: State of stress in the Conterminous United States: J. Geophys. Res., v. 85, p. 6113-6156.

MICHIGAN STATE UNIV LIBRARIES



31293108065750